Master's Thesis

Exploring 3 DOF upper limb dummy design method for upper limb impedance analysis

Jinsoo Kim

Department of Mechanical Engineering

Graduate School of UNIST

2020

Exploring 3 DOF upper limb dummy design method for upper limb impedance analysis

Jinsoo Kim

Department of Mechanical Engineering

Graduate School of UNIST

Exploring 3 DOF upper limb dummy design method for upper limb impedance analysis

A thesis/dissertation
submitted to the Graduate School of UNIST
in partial fulfillment of the
requirements for the degree of
Master of Science

Jinsoo Kim

6. 23. 2020 of submission

Approved by

Advisor
Sang Hoon Kang

Exploring 3 DOF upper limb dummy design method for upper limb impedance analysis

Jinsoo Kim

This certifies that the thesis/dissertation of Jinsoo Kim is approved.

6. 23. 2020 of submission

signature

Advisor: Sang Hoon Kang

signature

Namhun Kim: Thesis Committee Member #1

signature

Gwanseob Shin: Thesis Committee Member #2

Abstract

Patients with neurological diseases such as stroke are accompanied by joint construction, rigidity, and spasticity. This phenomenon can change the inherent mechanical properties of the muscles and tendons of the disabled upper extremities, and the mechanical impedance change of the upper extremities. An investigation was conducted to produce a dummy model of upper extremities to identify these mechanical impedance changes. First, the muscles affecting the shoulder and elbow joints in the upper extremities of the human body, parameters of muscles, and the main muscles in the direction of motion described in the existing literature were investigated. And then, the relative torque of individual muscles was calculated for imitating the major muscle muscles, and the priority of the muscles for each direction of motion was selected after comparison with the main muscles. In addition, through the existing literature, the muscles and extent of stiffness in stroke patients were investigated, and through expert advice, muscles were screened by excluding those with the same function but with little impact. For the development of spring-based upper limb dummy model, the upper limb muscle stiffness value was obtained by referring to the OpenSim platform model, and the parallel elastic element stiffness value of the muscle was obtained because the objective was to observe the passive movement of the muscle. Five postures were selected for the experiment, and the muscles where parallel elastic element stiffness was identified in each posture were investigated. Afterward, we checked the Origin & Insertion of each muscle to investigate inter-muscular interference and interference with the upper limb dummy, and to prevent interference by spreading the muscle in the direction of the moment-arm. The length of the upper limb dummy frame was based on Anthropometric Parameter, and the upper limb dummy design was carried out by reflecting the above points.

Contents

Figure contents

Table contents

I. Introduction

In the case of patients with neurological diseases such as stroke, neurological disorders affect several joints at the same time, accompanied by the construction, rigidity, and spasticity of several joints. These structural changes can cause changes in the inherent mechanical properties of the joints involved and can lead to contracture. The characteristics of muscles and tendons can be changed due to neurological disorders, and these changes in the characteristics of muscles and tendons can change the inherent mechanical properties of various joints in the disabled upper extremities. In addition, the mechanical impedance of end point due to the upper limb multiple joint, including the conjugated term between the joints, can be changed. Mechanical impedance is a relationship between the displacement applied to the upper limb and the resulting resistance force, and includes stiffness, viscosity, and inertia. In each joint, the individual joint impedance contributes to the multi-joint muscles, including mono-articular muscle and bi-articular muscle, and the coupled impedance between the joints becomes the contribution of the multi-joint muscles. These changes in the mechanical impedance of the upper limb multiple joints are well known in experience but are difficult to measure with clinical tests performed using the hands of the clinical workforce (Modified Ashworth Scale, Tardieu Scale, etc.). It is not possible to perform tests on two or more joints or degrees of freedom at the same time using both hands of the medical staff. Therefore, a repeatable and reliable estimation method of the impedance at the upper limb has been developed in order to grasp the change in the upper limb impedance due to the upper joint. In addition, many studies have performed mechanical impedance measurements on the upper limb 2 degrees of freedom (or 2 joints) (Mussa-Ivaldi, 1985; Dolan, 1993; Tsuji, 1995; Gomi, 1997; Acosta, 2000; Palazzolo, 2007), and in this study, the design of upper limb dummy models for estimating upper limb multi-joint impedance in three degrees of freedom space was explored.

II. Methods

2.1 Major muscles of shoulder and elbow joints

The purpose of this model is to measure mechanical impedance of both the shoulder and elbow joints (holding the wrist joints). Thus, muscles affecting shoulder and elbow joints were investigated based on anatomical books, and 11 shoulder muscles (Deltoid-anterior, Deltoid-medial, Deltoid-posterior, Supraspinatus, Infraspinatus, Subscapularis, Pectoralis major, Latissimus dorsi, Teres major, Teres minor, Coracobrachialis) and 9 elbow muscles(Biceps-long, Biceps-short, Brachioradialis, Brachialis, Triceps-long, Triceps-medial, Triceps-lateral, Pronator teres, Anconeus) were investigated (Palastanga, 2011; Stone, 2003; Perotto, 2011; Feneis, 2000). Then, to find out the main muscles of each joint, the relative torques of the individual muscles were investigated and found as follows (Braune, 1889).

$$\text{Relative torque of the individual muscle}(\%) = \frac{\text{Muscle Torque}(T_m)}{\text{Joint Torque}(\sum T_m)} \times 100 \quad (1)$$

Muscle Torque and Joint Torque represent the torques of individual and total muscles, respectively. To obtain Muscle Torque, use the following formula (Da Corte, 2014; Maganaris, 2000; Sacks, 1982).

$$\begin{aligned} \text{Muscle Torque}(T_m) &= \text{Muscle Force}(F_m) \times \text{Moment Arm(MA)} \\ &= \text{Specific tension} \times \text{PCSA} \times \cos(\alpha) \times \text{MA} \end{aligned} \quad (2)$$

$$\begin{aligned} \text{Muscle Force}(F_m) &= \text{Total Force}(F_f) \times \cos(\alpha) \\ &= \text{Specific tension} \times \text{PCSA} \times \cos(\alpha) \end{aligned} \quad (3)$$

$$\text{Total Force}(F_f) = \text{Specific tension} \times \text{PCSA} \quad (4)$$

Where PCSA is the physiological cross-sectional area and α is the pennation angle. Shoulder and elbow parameters measured by experiments in the existing literature (Specific tension, Physiological cross sectional area, Pennation angle, Moment arm) was investigated (Table 1, Table 2) (Kuechle, 1997, 2000; Favre, 2005; Veeger, 1991, 1997; Wood, 1989; Langenderfer, 2004; An, 1981; Murray, 1995, 2000, 2002; Amis, 1979), and the relative torque of the individual muscles shoulder and elbow movement direction in accordance with the above formula, each was calculated (Table 3). Specific tension was investigated as Elbow Flexor specific tension : 99~148 N/cm^2 , Elbow Extensor specific tension : 43~91 N/cm^2 , and Shoulder specific tension : 40~114 N/cm^2 (Buchanan, 1995; Wood, 1989; Chang, 2000; Crowninshield, 1981).

And compare the relative torque of the individual muscles calculated with the prime mover Muscle of the shoulder and elbow described in the existing literature (Lippert, 2011) (Table 4).

Base on the comparison between relative torque of the individual muscles and prime mover muscles results, exclude three muscles (Coracobrachialis, Pronator teres, Anconeus) that do not significantly affect the shoulder and elbow movement.

Subsequently, in order to identify the muscles that usually stiffen among the shoulder and elbow muscles, the botox injection site, one of the methods of spasticity treatment in the precedent research, is identified and reflected in the order of the muscles that are treated a lot (44 literature, 58 target groups) (Nalysnyk, 2013).

Table 1. Shoulder muscle parameter

	Physiological cross-sectional area (cm^2) [a]	Pennation angle (°)	Horizontal flexion Moment arm (cm) [b]	Abduction Moment arm (cm) [b]	Flexion Moment arm (cm) [b]	Rotation Moment arm (cm) [b]
Deltoid-anterior						
Kuechle (1997)	*	*	1.68	1.65	2.69	*
Kuechle (2000)	*	*	*	*	*	0.68
Favre (2005)	8.6	*	*	0.48	2.58	0
Veeger (1991)	*	*	*	*	*	*
Wood (1989)	4.52	*	*	*	*	*
Langenderfer (2004)	5.46	22	*	*	*	*
Deltoid-medial						
Kuechle (1997)	*	*	0.57	2.34	1.8	*
Kuechle (2000)	*	*	*	*	*	0.02
Favre (2005)	8.7	*	*	-2.07	0.67	0
Veeger (1991)	*	*	*	*	*	*
Wood (1989)	13.5	*	*	*	*	*
Langenderfer (2004)	7.39	15	*	*	*	*
Deltoid-posterior						
Kuechle (1997)	*	*	2.46	1.31	1.38	*
Kuechle (2000)	*	*	*	*	*	0.39
Favre (2005)	8.6	*	*	-1.98	2.88	0
Veeger (1991)	*	*	*	*	*	*
Wood (1989)	3.87	*	*	*	*	*
Langenderfer (2004)	4.69	29	*	*	*	*
Supraspinatus						
Kuechle (1997)	*	*	1.44	1.54	0.54	*
Kuechle (2000)	*	*	*	*	*	0.27
Favre (2005)	5.2	*	*	2.26	0.27	0.04
Veeger (1991)	5.21	*	*	*	*	*
Wood (1989)	4.5	*	*	*	*	*
Langenderfer (2004)	3.36	16	*	*	*	*
Infraspinatus						
Kuechle (1997)	*	*	1.86	0.23	0.1	*
Kuechle (2000)	*	*	*	*	*	2.34

Favre (2005)	9.6	*	*	0.73	0.2	1.9
Veeger (1991)	9.5	*	*	*	*	*
Wood (1989)	5.8	*	*	*	*	*
Langenderfer (2004)	8.34	18.5	*	*	*	*
Subscapularis						
Kuechle (1997)	*	*	0.3	0.56	0.39	*
Kuechle (2000)	*	*	*	*	*	2.18
Favre (2005)	13.5	*	*	0.29	0.73	1.85
Veeger (1991)	13.51	*	*	*	*	*
Wood (1989)	9.67	*	*	*	*	*
Langenderfer (2004)	9.49	20	*	*	*	*
Pectoralis major-clavicular						
Kuechle (1997)	*	*	4.05	4.65	1.01	*
Kuechle (2000)	*	*	*	*	*	1.84
Favre (2005)	4.6	*	*	0.87	2.87	0.62
Veeger (1991)	4.55	*	*	*	*	*
Wood (1989)	5.16	*	*	*	*	*
Langenderfer (2004)	3.07	17	*	*	*	*
Pectoralis major-sternal						
Kuechle (1997)	*	*	4.05	4.65	1.01	*
Kuechle (2000)	*	*	*	*	*	1.84
Favre (2005)	9.2	*	*	2.58	5.44	0.99
Veeger (1991)	9.1	*	*	*	*	*
Wood (1989)	8.39	*	*	*	*	*
Langenderfer (2004)	5.68	25	*	*	*	*
Latissimus dorsi						
Kuechle (1997)	*	*	0.36	3.67	3.65	*
Kuechle (2000)	*	*	*	*	*	0.82
Favre (2005)	8.7	*	*	4.9	0.57	0.66
Veeger (1991)	8.64	*	*	*	*	*
Wood (1989)	12.9	*	*	*	*	*
Langenderfer (2004)	7.3	21.6	*	*	*	*
Teres major						
Kuechle (1997)	*	*	0.36	4.65	4.6	*
Kuechle (2000)	*	*	*	*	*	0.67

Favre (2005)	10	*	*	4.15	1.28	0
Veeger (1991)	10	*	*	*	*	*
Wood (1989)	5.8	*	*	*	*	*
Langenderfer (2004)	2.93	16	*	*	*	*
Teres minor						
Kuechle (1997)	*	*	1.37	0.71	0.82	*
Kuechle (2000)	*	*	*	*	*	2
Favre (2005)	2	*	*	1.33	0.07	1.5
Veeger (1991)	2.92	*	*	*	*	*
Wood (1989)	2.58	*	*	*	*	*
Langenderfer (2004)	2.44	24	*	*	*	*
Coracobrachialis						
Kuechle (1997)	*	*	*	*	*	*
Kuechle (2000)	*	*	*	*	*	*
Favre (2005)	2.5	*	*	0.34	2.86	0
Veeger (1991)	2.51	*	*	*	*	*
Wood (1989)	1.29	*	*	*	*	*
Langenderfer (2004)	1.67	27	*	*	*	*

[a] PCSA values were calculated from other studies as follows: Favre: reported PCSA (average of the PCSA values found previous studies); Veeger: reported PCSA (PCSA was digitized); Wood: reported PCSA (muscle volume/muscle length); Langenderfer: reported PCSA (muscle volume/optimal fascial length).

[b] Moment arm values were measured at the following angles: Kuechle (1997): 0°~140° horizontal flexion, 0°~90° abduction and 0°~80° flexion; Kuechle (2000): -60°~60° neutral position rotation; Favre (2005): 0°, 30°, 60°, 80° abduction and -30°, 0°, 30° flexion and -60°, 0° rotation.

Table 2.Elbow muscle parameter

	Physiological cross-sectional area (cm^2) [a]	Pennation angle (°)	Moment arm (cm) [b]
Biceps-long			
Wood (1989)	1.94	*	*
Veeger (1991)	3.21	*	*
Veeger (1997)	2.78	<15	*
Langenderfer (2004)	1.57	0	*
An (1981)	2.5	*	*
Murray (1995)	*	*	4
Murray(2000)	2.5	0	4.7
Murray (2002)	*	*	4.2~5.4
Amis (1979)	4.1	0	*

Biceps-short			
Wood (1989)	1.29	*	*
Veeger (1991)	3.08	*	*
Veeger (1997)	2.56	<15	*
Langenderfer (2004)	1.75	0	*
An (1981)	2.1	*	*
Murray (1995)	*	*	4
Murray(2000)	2.1	0	4.7
Murray (2002)	*	*	4.2~5.4
Amis (1979)	4.1	0	*
Brachioradialis			
Wood (1989)	1.29	*	*
Veeger (1991)	*	*	*
Veeger (1997)	2.87	<15	*
Langenderfer (2004)	1.15	0	*
An (1981)	1.5	*	*
Murray (1995)	*	*	6
Murray(2000)	1.2	0	7.7
Murray (2002)	*	*	7~9
Amis (1979)	3.2	0	*
Brachialis			
Wood (1989)	9	*	*
Veeger (1991)	*	*	*
Veeger (1997)	5.6	<15	*
Langenderfer (2004)	7.71	18	*
An (1981)	7	*	*
Murray (1995)	*	*	2.5
Murray(2000)	5.4	0	2.6
Murray (2002)	*	*	2.1~3
Amis (1979)	9.4	0	*
Triceps long			
Wood (1989)	3.9	*	*
Veeger (1991)	6.8	*	*
Veeger (1997)	4.7	30	*
Langenderfer (2004)	3.6	12	*
An (1981)	6.7	*	*
Murray (1995)	*	*	2.5

Murray(2000)	4.3	10	2.3
Murray (2002)	*	*	1.8~2.8
Triceps medial			
Wood (1989)	3.2	*	*
Veeger (1991)	6.8	*	*
Veeger (1997)	5.25	45	*
Langenderfer (2004)	3.21	17	*
An (1981)	6.1	*	*
Murray (1995)	*	*	2.5
Murray(2000)	4.5	8	2.3
Murray (2002)	*	*	1.8~2.8
Triceps lateral			
Wood (1989)	4.5	*	*
Veeger (1991)	6.8	*	*
Veeger (1997)	3.83	30	*
Langenderfer (2004)	4.13	26	*
An (1981)	6	*	*
Murray (1995)	*	*	2.5
Murray(2000)	4.5	8	2.3
Murray (2002)	*	*	1.8~2.8
Pronator teres			
Wood (1989)	*	*	*
Veeger (1991)	*	*	*
Veeger (1997)	1.7	<15	*
Langenderfer (2004)	*	*	*
An (1981)	3.4	*	*
Murray (1995)	*	*	2.5
Murray(2000)	2.8	13	1.7
Murray (2002)	*	*	1.3~2
Amis (1979)	4.4	5-9	*
Anconeus			
Wood (1989)	*	*	*
Veeger (1991)	*	*	*
Veeger (1997)	1.24	30	*
Langenderfer (2004)	*	*	*
An (1981)	2.5	*	*
Murray (1995)	*	*	*

Murray(2000)	*	*	*
Murray (2002)	*	*	*

[a] PCSA values were calculated from other studies as follows: Wood: reported PCSA (muscle volume/muscle length); Veeger (1991): reported PCSA (PCSA was digitized); Veeger (1997): reported PCSA (muscle volume/muscle length); Langenderfer: reported PCSA (muscle volume/optimal fascial length); An: reported PCSA (muscle volume/fiber length); Murray (2000): reported PCSA (muscle volume/optimal fascial length); Amis: muscle weight/fiber length * 1.06;

[b] Moment arm values were measured at the following angles: Murray (1995): 25°~110° flexion for elbow flexors and 35°~120° flexion for triceps; Murray (2000, 2002): 20°~120° flexion for elbow flexors and 30°~120° flexion for triceps;

Table 3. Relative torque of the individual muscles (Percentage indicates muscle contribution to the overall torque of each movement)

Shoulder Horizontal Abduction	Shoulder Horizontal Adduction	Shoulder Abduction	Shoulder Adduction	Shoulder Flexion	Shoulder Extension	Shoulder Internal rotation	Shoulder External rotation	Elbow Flexion	Elbow Extension
Infraspinatus (30.89%)	Pectoralis major (78.49%)	Deltoid-medial (53.54%)	Latissimus dorsi (30.69%)	Pectoralis major-sternal (39.55%)	Teres major (32.04%)	Subscapularis (45.24%)	Infraspinatus (74.37%)	Brachialis (32.87%)	Triceps-long (32.46%)
Deltoid-Posterior (25.94%)	Deltoid-Anterior (16.1%)	Supraspinatus (21.24%)	Teres major (24.89%)	Deltoid-anterior (25.33%)	Latissimus dorsi (29.09%)	Pectoralis major-sternal (21.42%)	Teres minor (17.71%)	Biceps-long (20%)	Triceps-lateral (31.44%)
Supraspinatus (13.32%)	Subscapularis (5.42%)	Deltoid-anterior (15.62%)	Pectoralis major-sternal (21.73%)	Pectoralis major-clavicular (13.48%)	Deltoid-medial (18.6%)	Latissimus dorsi (13.34%)	Deltoid-posterior (4.45%)	Brachioradialis (18.71%)	Triceps-medial (30.25)
Deltoid-medial (11.44%)		Infraspinatus (9.61%)	Pectoralis major-clavicular (9.35%)	Subscapularis (10.75%)	Deltoid-posterior (16.83%)	Pectoralis major-clavicular (10.56%)	Supraspinatus (3.03%)	Biceps-short (18.03%)	Anconeus (5.84%)
Latissimus dorsi (6.57%)			Deltoid-Posterior (6.76%)	Coracobrachialis (8.48%)	Infraspinatus (1.86%)	Teres major (4.85%)	Deltoid-medial (0.45%)	Pronator teres (10.39%)	
Teres minor (6.57%)			Subscapularis (4.18%)	Supraspinatus (3.01%)	Teres minor (1.61%)	Deltoid-anterior (4.03%)			
Teres			Teres						

major (5.23%)	minor (1.9%) Coracobrachialis (0.49%)	

Table 4. Compare the prime mover muscles described in the Kinesiology book and relative torque of the individual muscles through each movement.

	Relative torque of the individual muscle	Clinical Kinesiology and Anatomy (2011)
Shoulder Horizontal Abduction	Infraspinatus (30.89%) Deltoid-Posterior (25.94%) Supraspinatus (13.32%) Deltoid-medial (11.44%) Latissimus dorsi (6.57%) Teres minor (6.57%) Teres major (5.23%)	Infraspinatus Deltoid-posterior Teres minor
Shoulder Horizontal Adduction	Pectoralis major (78.49%) Deltoid-Anterior (16.1%) Subscapularis (5.42%)	Pectoralis major-clavicular Deltoid-anterior
Shoulder Abduction	Deltoid-medial (53.54%) Supraspinatus (21.24%) Deltoid-anterior (15.62%) Infraspinatus (9.61%)	Deltoid-medial, anterior, posterior Supraspinatus
Shoulder Adduction	Latissimus dorsi (30.69%) Teres major (24.89%) Pectoralis major-sternal (21.73%), Pectoralis major-clavicular (9.35%) Deltoid-Posterior (6.76%) Subscapularis (4.18%) Teres minor (1.9%) Coracobrachialis (0.49%)	Latissimus dorsi Teres major Pectoralis major
	Pectoralis major-sternal (39.55%),	Pectoralis major-clavicular (0°~60°)

Shoulder Flexion	Pectoralis major-clavicular (13.48%) Deltoid-anterior (25.33%) Subscapularis (10.75%) Coracobrachialis (8.48%) Supraspinatus (3.01%)	Deltoid-anterior
Shoulder Extension	Teres major (32.04%) Latissimus dorsi (29.09%) Deltoid-medial (18.6%) Deltoid-posterior (16.83%) Infraspinatus (1.86%) Teres minor (1.61%)	Teres major Latissimus dorsi Deltoid-posterior Pectoralis major-sternal (120°~180°)
Shoulder Internal rotation	Subscapularis (45.24%) Pectoralis major-sternal (21.42%) Pectoralis major-clavicular (10.56%) Latissimus dorsi (13.34%) Teres major (4.85%) Deltoid-anterior (4.03%)	Subscapularis Pectoralis major Latissimus dorsi Teres major Deltoid-anterior
Shoulder External rotation	Infraspinatus (74.37%) Teres minor (17.71%) Deltoid-posterior (4.45%) Supraspinatus (3.03%) Deltoid-medial (0.45%)	Infraspinatus Teres minor Deltoid-posterior
Elbow Flexion	Brachialis (32.87%) Biceps-long (20%) Brachioradialis (18.71%) Biceps-short (18.03%) Pronator teres (10.39%)	Brachialis Biceps-long, short Brachioradialis
Elbow Extension	Triceps-long (32.46%) Triceps-lateral (31.44%) Triceps-medial (30.25%) Anconeus (5.84%)	Triceps-long, lateral, medial

It was confirmed that botox is mainly injected into 3 shoulder muscles (Infraspinatus, Subscapularis, Pectoralis major) and 4 elbow muscles (Biceps brachii, Brachialis, Brachioradialis, Triceps brachii),

which means that these muscles are mainly stiff muscles.

In addition, the muscles used in the 2 DOF biomechanical arm model (Jagodnik, 2010; Zadravec, 2013; Sharifi, 2017) introduced in the precedent research were investigated (Table 5).

Table 5. 2 DOF Biomechanical arm model design and muscles used in each model.

2 DOF Biomechanical arm model	
Deltoid anterior Deltoid posterior Triceps long Triceps medial Triceps lateral Biceps brachii Brachialis	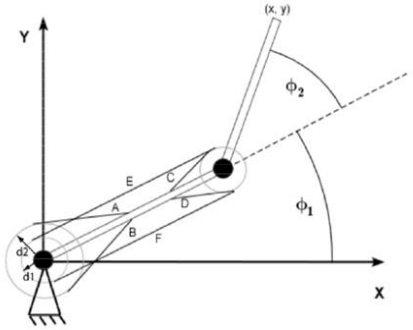 Jagodnik, 2010
Pectoralis major Deltoid posterior Triceps long Triceps lateral Biceps-brachii Brachialis	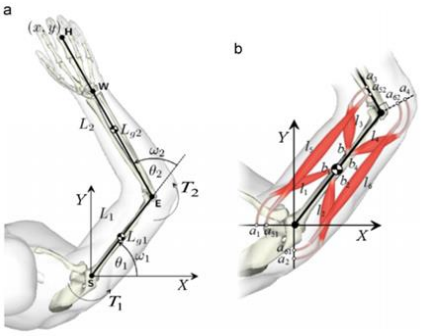 Zadravec, 2013
Deltoid anterior Deltoid posterior Triceps long Triceps lateral Biceps long Brachialis	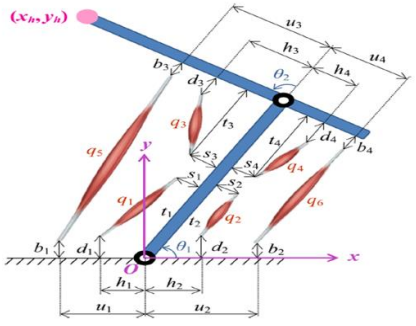 Sharifi, 2017

Afterwards, an expert advisory meeting was held based on the muscles investigated, and through this, three additional muscles (Teres major, Teres minor, Triceps-lateral) were excluded. The criteria for selecting excluded muscles perform the same function, but because of their small size, less effective muscles are excluded. Teres major is a muscle that performs medial rotation, adduction, and extension

exercises, and performs the same action as Latissimus dorsi, but its size is much smaller and less effective, so it is excluded (Lippert, 2011; Carol A, 2016). Teres minor is a muscle that performs lateral rotation, horizonal abduction, and extension exercises that perform the same actions as Infraspinatus, but was excluded because physiological cross-sectional area is smaller than Infraspinatus and can apply only a little extra force to the lateral rotation (Floyd, 2017; Carol A, 2016). Triceps-lateral performs the same actions as Triceps-Medial, but Triceps-lateral is activated only when the demand for force increases, and Triceps-Medial is mostly activated in the operating range. Therefore, Triceps-lateral was excluded (Carol A, 2016; Foster, 2019).

Thus, a total of 14 muscles were finally selected, with eight shoulder muscles (Infraspinatus, Deltoid-anterior, Deltoid-medial, Deltoid-posterior, Pectoralis major, Supraspinatus, Latissimus dorsi, Subscapularis) and six elbow muscles (Brachialis, Biceps-long, Biceps-short, Brachioradialis, Triceps-long, Triceps-medial). The selected muscles for each exercise are arranged in the table below (Table 6).

Table 6. Final selection muscle (A total of 14 muscles are selected from muscles including Relative torque & prime mover, Botox injection, and 2 DOF biomechanical arm model muscles, excluding those with low contribution or overlapping functions).

	Relative torque & Prime mover	Botox injection	2 DOF Biomechanical arm model	Final selection muscle (14 total)
Shoulder Horizontal Abduction	Infraspinatus Deltoid-posterior	Infraspinatus	Deltoid anterior Deltoid posterior Pectoralis major	①Infraspinatus ②Deltoid-posterior
Horizontal Adduction	Pectoralis major-clavicular Deltoid-anterior	Pectoralis major		③Pectoralis major ④Deltoid-anterior
Abduction	Deltoid-medial Deltoid-anterior Deltoid-posterior Supraspinatus			⑤Deltoid-medial Deltoid-anterior Deltoid-posterior ⑥Supraspinatus
Adduction	Latissimus dorsi Teres major Pectoralis major			⑦Latissimus dorsi Pectoralis major

Flexion	Pectoralis major-clavicular Deltoid-anterior	Pectoralis		Pectoralis major Deltoid-anterior
Extension	Teres major Latissimus dorsi Deltoid-posterior			Latissimus dorsi Deltoid-posterior
Internal rotation	Subscapularis Pectoralis major Latissimus dorsi Teres major Deltoid-anterior	Subscapularis Pectoralis		⑧Subscapularis Pectoralis major Deltoid-anterior
External rotation	Infraspinatus Teres minor Deltoid-posterior	Infraspinatus		Infraspinatus Deltoid-posterior
Elbow Flexion	Brachialis Biceps-long Biceps-short Brachioradialis	Brachialis Biceps brachii Brachioradialis	Biceps brachii Brachialis Triceps-long Triceps-medial Triceps-lateral	⑨Brachialis ⑩Biceps-long ⑪Biceps-short ⑫Brachioradialis
Extension	Triceps-long Triceps-lateral Triceps-medial	Triceps brachii		⑬Triceps-long ⑭Triceps-medial

2.2 Experiment posture

Five positions are selected for impedance measurement. First, the posture of zero resistance torque in shoulder horizontal adduction/abduction and elbow flexion/extension movements was confirmed by referring to the previous studies (Ren, 2012). Resistance torque becomes zero when shoulder horizontal adduction is 65° and elbow flexion is 60°. In addition, the maximum angle of shoulder abduction that can be applied without force is confirmed by the robot system currently in the laboratory. It was confirmed that the shoulder abduction angle was 40° for men (height 179cm) and 50° for women (height 159cm), and it was decided to be 25° smaller than 40°, the maximum angle for shoulder abduction angle (Figure 1). The shoulder and elbow movements are as shown (Figure 2).

Therefore, the posture for the impedance measurement is set to shoulder abduction 25°, shoulder horizontal adduction 65°, and elbow flexion 60°. When viewing the basic impedance measurement

posture from side, the shoulder flexion angle is 45°.

After that, the final five positions were selected by adding two positions with a change of ±15° from the shoulder flexion angle of 45° and two positions with a change of ±10° from the shoulder abduction angle of 25° (Figure 3). The shoulder external rotation angle is obtained by calculating the coordinates of the wrist marker based on the shoulder point when each position is taken using motion capture (Table 7).

The range of motion for each posture is defined as Shoulder abduction ± 5°, Shoulder flexion ± 5°, and Shoulder external rotation ± 5°.

(A)

(B)

Figure 1. Check the maximum shoulder abduction angle that the robot system can take. (A) Maximum shoulder abduction angle of the male(179cm) is 40°. (B) Maximum shoulder abduction angle of the female(159cm) is 50°

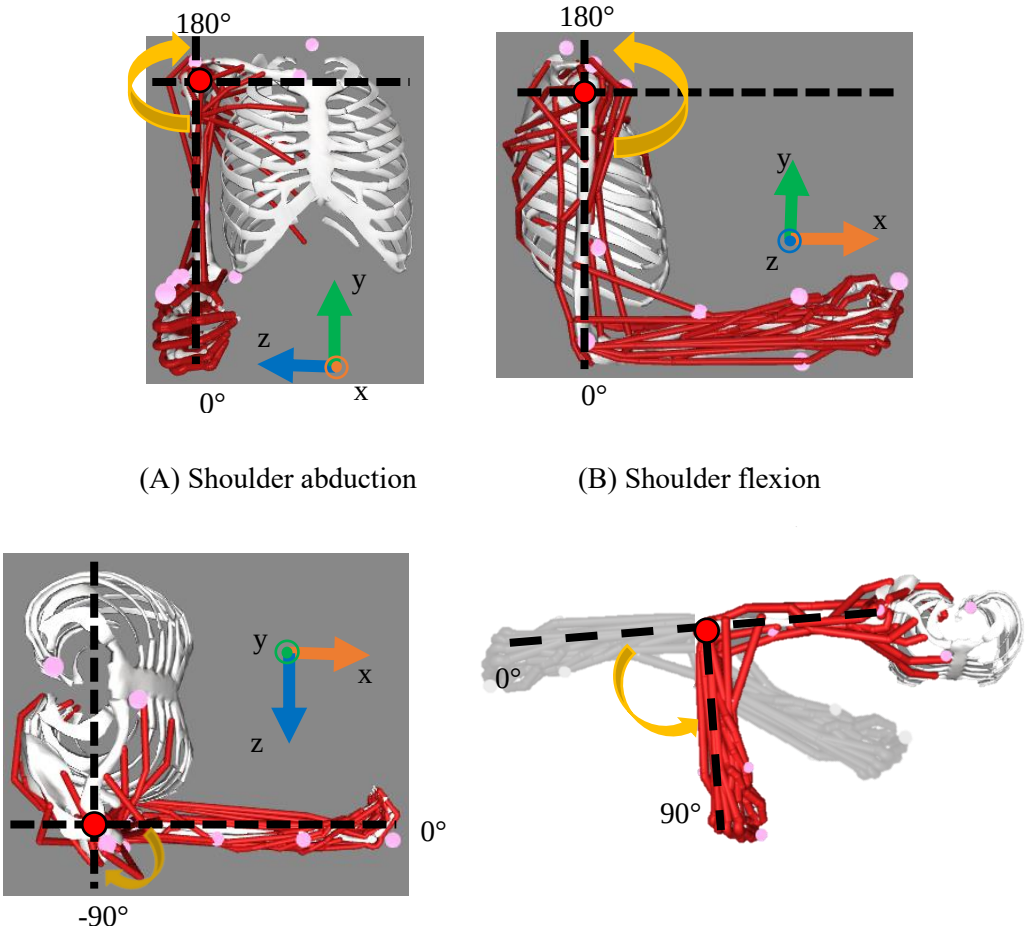

Figure 2. Shoulder and elbow motion. (A) Shoulder abduction axis and direction of movement during shoulder abduction. (B) Shoulder flexion axis and direction of movement during shoulder flexion. (C) Shoulder external rotation axis and direction of movement during shoulder external rotation. (D) Elbow flexion axis and direction of movement during elbow flexion.

Table 7. Angle of selected posture

Posture	Shoulder abduction (°)	Shoulder flexion (°)	Shoulder external rotation (°)	Elbow flexion (°)
1 (Reference)	25	45	-57.95	60
2	25	60	-71.71	60
3	25	30	-43.31	60
4	35	45	-54.37	60
5	15	45	-61.02	60

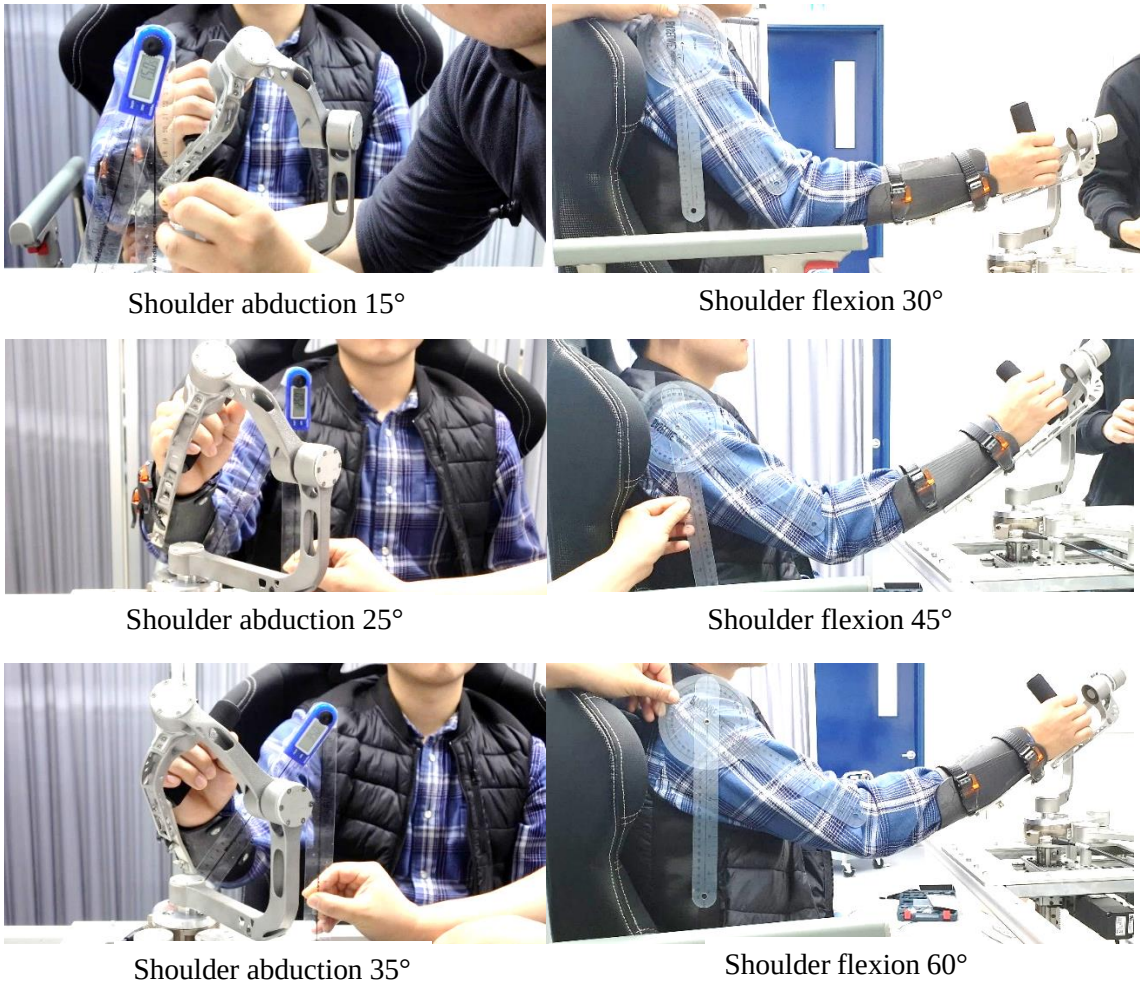

Figure 3. Actual appearance at shoulder abduction angles of 25° and ±5°, and actual appearance at shoulder flexion reference angles of 45° and ±5°.

2.3 Design method for muscles

The stiffness of the muscle will be investigated to develop a spring-based upper limb dummy model. The purpose of this study was to observe the passive movement of muscles, so the value of passive stiffness of muscles was determined. Passive stiffness can be defined as the resistance to elongation or shortening or, in physical terms, the change in tension per unit change in length. In case of muscle, the connective tissue that surrounds the contractile element influences the force-length curve. It is called the parallel elastic component, and it acts much like an elastic band. When the muscle is at resting length or less, the parallel elastic component is in a slack state with no tension. As the muscle lengthens, the parallel element is no longer loose, so tension begins to build up, slowly at first and then more rapidly.

At this time, the parallel element generates passive force, and the parallel elastic element stiffness value that causes passive force is passive stiffness (Figure 4).

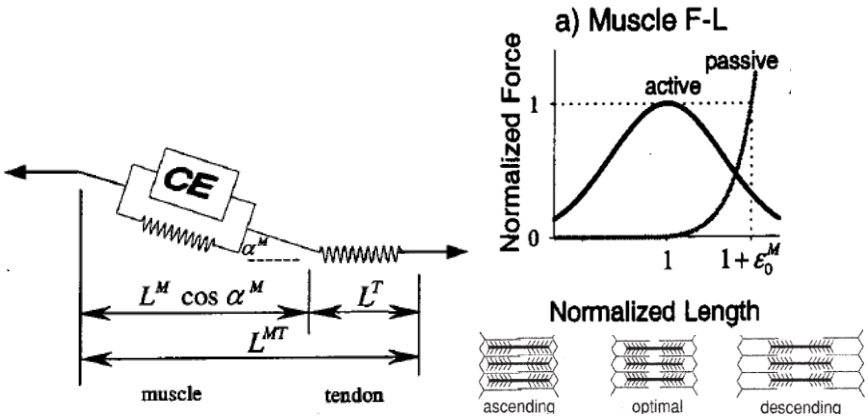

Figure 4. A Hill-type model was used to describe musculo-tendon contraction mechanics. The model consists of a muscle contractile element in series and parallel with elastic elements. Contractile element make active force and parallel elastic element make passive force.

The passive force-length relationship of muscle is represented by a following function. (Thelen, 2003).

$$\overline{F}^{PE} = \frac{e^{k^{PE}(\overline{L^M}-1)/\varepsilon_o^M} - 1}{e^{k^{PE}} - 1} \tag{5}$$

Where $\overline{F}^{PE}$ is the normalized passive muscle force, $\overline{L}^M$ is the normalized muscle fiber length, k^{PE} (=4) is the shape factor, ε_o^M (=0.6) is the parallel elastic element stiffness due to maximum isometric force (Thelen, 2003). Passive force and fiber length are normalized to maximum isometric muscle force (F_o^M) and optimal muscle fiber length (L_o^M), respectively.

$$\begin{aligned} \overline{F}^{PE} &= F^{PE} / F_o^M \\ \overline{L}^M &= L^M / L_o^M \end{aligned} \tag{6}$$

The above equation can be summarized as a parallel elastic element stiffness equation.
The maximum isometric muscle force and optimal fiber length are referred to in the previous paper (Saul, 2015) (Table 8).

$$\frac{dF^{PE}}{dL^M} = \frac{F_o^M k^{PE} e^{\frac{k^{PE}(\frac{L^M}{L_o^M}-1)}{\varepsilon_o^M}}}{L_o^M \varepsilon_o^M (e^{k^{PE}} - 1)} \quad (7)$$

Table 8. Optimal fiber length and Maximum isometric muscle forces

	Muscle	Optimal fiber length (L_o^M) [a], [m]	Maximum isometric muscle force (F_o^M), [N]
Shoulder	Infraspinatus	0.0755	1075.8
	Subscapularis	0.0873	1306.9
	Pectoralis major-clavicular	0.1442	444.3
	Pectoralis major-sternal	0.1385	658.3
	Pectoralis major-ribs	0.1385	498.1
	Deltoid-anterior	0.0976	1218.9
	Deltoid-medial	0.1078	1103.5
	Deltoid-posterior	0.1367	201.6
	Latissimus dorsi-Thoracic	0.254	290.5
	Latissimus dorsi-Lumbar	0.2324	317.5
	Latissimus dorsi-Iliac	0.2789	189
	Supraspinatus	0.0682	499.2
Elbow	Triceps-long	0.134	771.8
	Triceps-medial	0.1138	717.5
	Biceps-long	0.1157	525.1
	Biceps-short	0.1321	316.8
	Brachialis	0.0858	1177.37
	Brachioradialis	0.1726	276.0

[a] Fiber lengths were normalized to an optimal sarcomere length of 2.7 μm. Peak force is calculated as the product of physiological cross-sectional area (PCSA) and specific tension (specific tension of 140 N cm^{-2} for muscles of the elbow and shoulder).

In addition, spring design imitating patient muscles was required for impedance analysis of stroke patients, and to this end, the rate of decrease in patient optimal fiber length was identified. According to previous papers, the optimal fiber length reduction rate of patients was found to be 19.7% for biceps brachii and 15.9% for triceps brachii (Nelson, 2018). The rate of decrease in the optimal fiber length of the muscles not specified is specified at 17.8%, the average of the two values.

2.4 Muscle interference and solution

When manufacturing the upper limb dummy, problems may occur if the origin & insertion position of the actual muscle is used as it is. This is because the actual muscles may be intertwined or covered by other muscles. To confirm this, we made a simple mockup of the upper limb and identified the problem. (Figure 5).

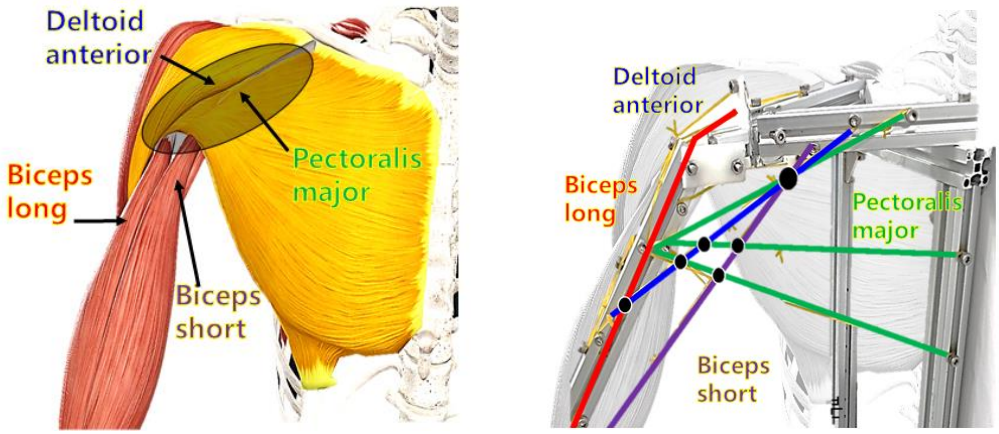

(A) (B)

Figure 5. (A) The inter-muscular interference of the front of the human shoulder. (B) The inter-muscular(spring) interference of the upper limb dummy.

If the origin & insertion position of the actual muscle is applied to the upper limb dummy as described above, interference may occur between the springs, and this causes resistance and friction, which prevents proper experimentation. As a solution to this, the distance between the origin and insertion of the muscle is given to prevent interference between the muscles. If the Origin & Insertion of the muscle is given a distance, the moment has the following relationship with the moment of the existing muscle (Figure 6).

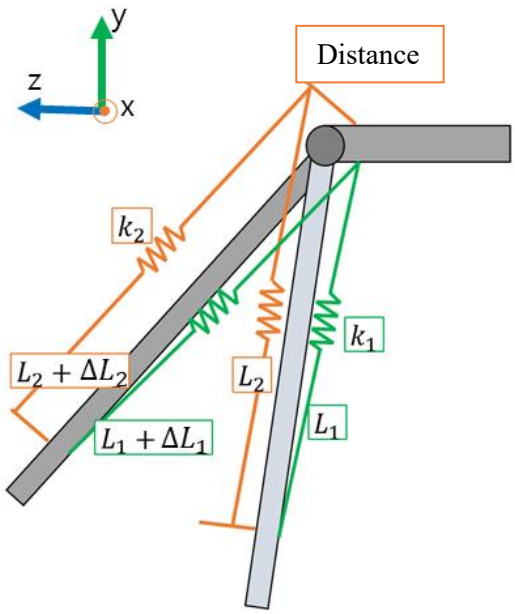

Figure 6. The normal muscle (green line) and the distance-given muscle (orange line) are attached based on the joint

$$\begin{bmatrix} M_{x_1} \\ M_{y_1} \\ M_{z_1} \end{bmatrix} = \begin{bmatrix} r_{x_1} & r_{y_1} & r_{z_1} \end{bmatrix} \times k_1 \begin{bmatrix} \Delta L_{x_1} \\ \Delta L_{y_1} \\ \Delta L_{z_1} \end{bmatrix} \text{ Original moment} \tag{8}$$

$$\begin{bmatrix} M_{x_2} \\ M_{y_2} \\ M_{z_2} \end{bmatrix} = \begin{bmatrix} r_{x_2} & r_{y_2} & r_{z_2} \end{bmatrix} \times k_2 \begin{bmatrix} \Delta L_{x_2} \\ \Delta L_{y_2} \\ \Delta L_{z_2} \end{bmatrix} \text{ Distance-given moment} \tag{9}$$

$$\begin{aligned} \overrightarrow{M_i} &= \vec{r_i} \times \overrightarrow{F_i} \\ \overrightarrow{F_i} &= k_i \Delta \overrightarrow{L_i} \end{aligned} \tag{10}$$

Where M_i is the moment, r_i is the moment arm, F_i is the force, k_i is the muscle stiffness, L_i is the muscle length, ΔL_i is the muscle length variation. Here we find the value of k_2 so that original moment and distance-given moment have similar values. First of all, in order to have the same direction of the moment applied to the joint, the distance must be given in the direction of the moment arm.

To know the direction of the moment arm, the coordinates of the moment arm are required and can be obtained in the following way (Figure 7).

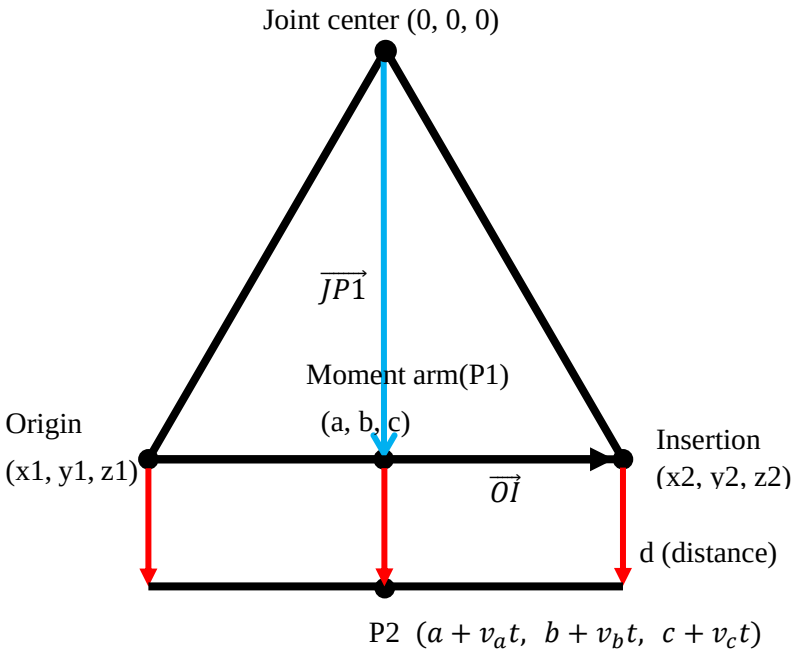

Figure 7. A description of the joint center, origin & insertion, moment arm, and distance-given moment arm coordinates

$$\begin{aligned} \overrightarrow{JP1} &= (a,b,c) \\ \overrightarrow{OI} &= (x_2 - x_1,\ y_2 - y_1,\ z_2 - z_1) \end{aligned} \tag{11}$$

$$\left(\frac{x_2 - x_1}{\sqrt{(x_2 - x_1)^2 + (y_2 - y_1)^2 + (z_2 - z_1)^2}}, \frac{y_2 - y_1}{\sqrt{(x_2 - x_1)^2 + (y_2 - y_1)^2 + (z_2 - z_1)^2}}, \frac{z_2 - z_1}{\sqrt{(x_2 - x_1)^2 + (y_2 - y_1)^2 + (z_2 - z_1)^2}}\right)$$

$$= \left(\frac{x_2 - x_1}{v}, \frac{y_2 - y_1}{v}, \frac{z_2 - z_1}{v}\right) = (v_x, v_y, v_z) \qquad \left(v = \sqrt{(x_2 - x_1)^2 + (y_2 - y_1)^2 + (z_2 - z_1)^2}\right) \tag{12}$$

Using the above equation, we find the direction vector from the origin coordinate to the insertion coordinate. After that, set the coordinates of the moment arm as below.

$$a = x_1 + v_x t_{OI},\ \ b = y_1 + v_y t_{OI},\ \ c = z_1 + v_z t_{OI} \tag{13}$$

Where t_{OI} is a multiple multiplied by the $\overrightarrow{OI}$ direction vector. When the two straight lines are vertical, the dot product of the two straight lines becomes zero, so the following equation can be obtained.

$$\begin{aligned} &\overrightarrow{JP1} \cdot \overrightarrow{OI} = 0 \\ &a(x_2 - x_1) + b(y_2 - y_1) + c(z_2 - z_1) = 0 \end{aligned} \tag{14}$$

The above equation can be summarized as an equation about t_{OI} as follows.

$$t_{OI}\left(\frac{(x_2-x_1)^2}{v}+\frac{(y_2-y_1)^2}{v}+\frac{(z_2-z_1)^2}{v}\right)+x_1(x_2-x_1)+y_1(y_2-y_1)+z_1(z_2-z_1)=0$$
$$t_{OI}=-\frac{x_1(x_2-x_1)+y_1(y_2-y_1)+z_1(z_2-z_1)}{v}=-\frac{x_1(x_2-x_1)+y_1(y_2-y_1)+z_1(z_2-z_1)}{\sqrt{(x_2-x_1)^2+(y_2-y_1)^2+(z_2-z_1)^2}} \quad (15)$$

Here, the values of v_x, v_y, v_z and t_{OI} can be found to find the coordinates of the moment arm. And the direction vector of the moment arm can be known using the coordinates of the moment arm. Through this, the distance can be calculated in the following equation.

$$\left(\frac{a}{\sqrt{a^2+b^2+c^2}},\frac{b}{\sqrt{a^2+b^2+c^2}},\frac{c}{\sqrt{a^2+b^2+c^2}}\right)=(v_a,v_b,v_c) \quad (16)$$

Use the above equation to find the direction vector of the moment arm.

$$P_2=(a+v_at_{P12},b+v_bt_{P12},c+v_ct_{P12}) \quad (17)$$

P_2 is the coordinate of the moment arm that gave the distance, and t_{P12} is the multiplier of the $\overrightarrow{OI}$ direction vector. Here, the distance D is adjusted by changing the t_{P12} value using the following relationship.

$$d=\sqrt{(v_at_{P12})^2+(v_bt_{P12})^2+(v_ct_{P12})^2}$$
$$t_{P12}=\frac{d}{\sqrt{(v_a{}^2+v_b{}^2+v_c{}^2)}} \quad (18)$$

Using the above equation, give a distance so that the muscles do not overlap, calculate the moment, and obtain the k_2 value by comparing it with the moment value of the muscle before giving the distance. The origin and insertion coordinates of the muscle refer to the coordinates of the OpenSim model (Holzbaur, 2005).

2.5 Model parameter

The upper limb dummy model consists of clavicle, scapula, humerus, radius, and ulna because it

observes shoulder and elbow movements. The clavicle and scapula are fixed parts without movement, so the two parts are combined to designate the frame. Also, the pronation/supination movement is not considered in this study, so two parts of radius and ulna are considered as one part. The lengths of the humerus (291 mm) and radius & ulna (258 mm) are consistent with published data describing a 50th percentile male (170 cm tall) (McConville, 1980; Saul, 2015).

III. Results

3.1 Muscle interference results and distance values

To identify the muscles where interference occurs, the muscles that show passivity for each position are identified. Parallel elastic element stiffness appears when muscle fiber length is longer than optimal fiber length.

The fiber length when the previously selected muscles were moved by a specified range of motion for each posture is examined. Fiber length values are obtained using the OpenSim model (Holzbaur, 2005). Summarize the muscles with parallel elastic element stiffness is identified when moved by the specified range of motion for each position (Table 9, 10).

The result is true when the movement is ±5° for each motion (shoulder abduction, shoulder flexion, shoulder external rotation, elbow flexion) in a total of 5 postures.

Table 9. Muscles where parallel elastic element stiffness is measured in each posture

Motion	Reference posture	Posture 2	Posture 3	Posture 4	Posture 5
Shoulder abduction	Infraspinatus Deltoid-posterior	Deltoid-posterior	Infraspinatus Deltoid-anterior	Deltoid-posterior	Infraspinatus Deltoid-posterior
Shoulder flexion	Infraspinatus Deltoid-posterior	Deltoid-posterior	Infraspinatus Deltoid-anterior	Deltoid-posterior	Infraspinatus Deltoid-posterior

Shoulder external rotation	Infraspinatus Deltoid-posterior	Deltoid-posterior	Infraspinatus Deltoid-anterior	*	Infraspinatus Deltoid-posterior
Elbow flexion	Triceps-long Biceps-long Biceps-short	Triceps-long Biceps-long Biceps-short	Triceps-long Biceps-long Biceps-short	Triceps-long Biceps-long Biceps-short	Triceps-long Biceps-long Biceps-short

Table 10. Muscles where parallel elastic element stiffness is measured in each posture (apply patient optimal fiber length)

Motion	Reference posture	Posture 2	Posture 3	Posture 4	Posture 5
Shoulder abduction	Infraspinatus Deltoid-posterior Subscapularis Pectoralis major-clavicular	Infraspinatus Deltoid-posterior Subscapularis	Infraspinatus Deltoid-anterior Subscapularis Pectoralis major-clavicular	Infraspinatus Deltoid-posterior Subscapularis Pectoralis major-clavicular	Infraspinatus Deltoid-posterior Subscapularis
Shoulder flexion	Infraspinatus Deltoid-posterior Subscapularis Pectoralis major-clavicular	Infraspinatus Deltoid-posterior Subscapularis	Infraspinatus Deltoid-anterior Subscapularis Pectoralis major-clavicular	Infraspinatus Deltoid-posterior Subscapularis Pectoralis major-clavicular	Infraspinatus Deltoid-posterior Subscapularis
Shoulder external rotation	Infraspinatus Deltoid-posterior Subscapularis Pectoralis major-clavicular	Infraspinatus Deltoid-posterior Subscapularis	Infraspinatus Deltoid-anterior Subscapularis Pectoralis major-clavicular	Infraspinatus Subscapularis Pectoralis major-clavicular	Infraspinatus Deltoid-posterior Subscapularis
Elbow flexion	Triceps-long Biceps-long Biceps-short Brachialis Brachioradialis	Triceps-long Biceps-long Biceps-short Brachialis Brachioradialis	Triceps-long Biceps-long Biceps-short Brachialis Brachioradialis	Triceps-long Biceps-long Biceps-short Brachialis Brachioradialis	Triceps-long Biceps-long Biceps-short Brachialis Brachioradialis

Origin and Insertion of muscles for each posture were connected to check interference, and it was confirmed that interference between Infraspinatus and Triceps-long muscles occurred in all postures. Infraspinatus is given a 5mm distance in the direction of the moment arm to avoid interference between the two muscles (Figure 8).

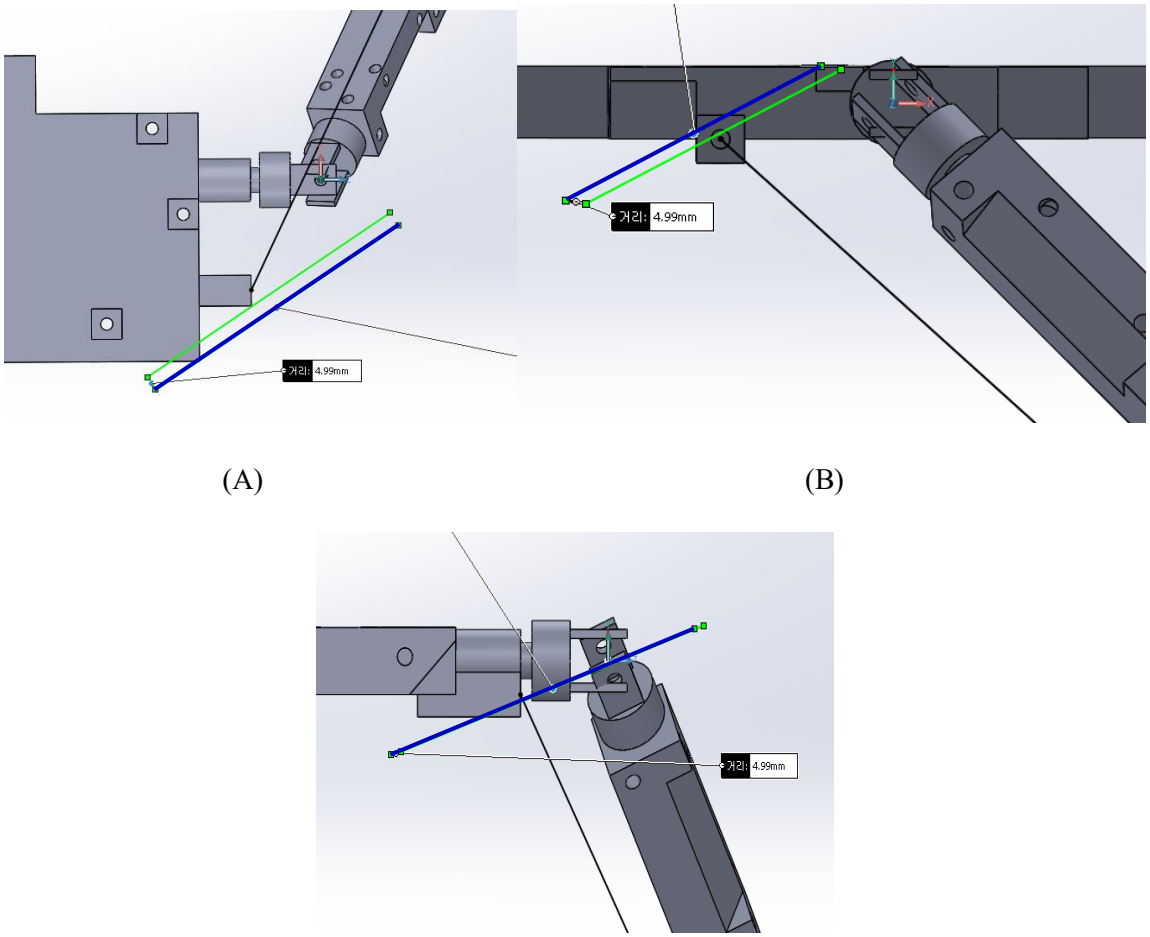

(A) (B)

(C)

Figure 8. Triceps-long (black line), Infraspinatus (green line), Distance-given (5mm) infraspinatus (blue line) in reference posture. (A) Top view. (B) Right side view. (C) Back side view.

In addition, it was confirmed that the interference between the Deltoid-posterior and the upper limb dummy occurred in the posture 2, and for this purpose, a 6mm distance was applied to the Deltoid-posterior muscle in the posture 2. (Figure 9).

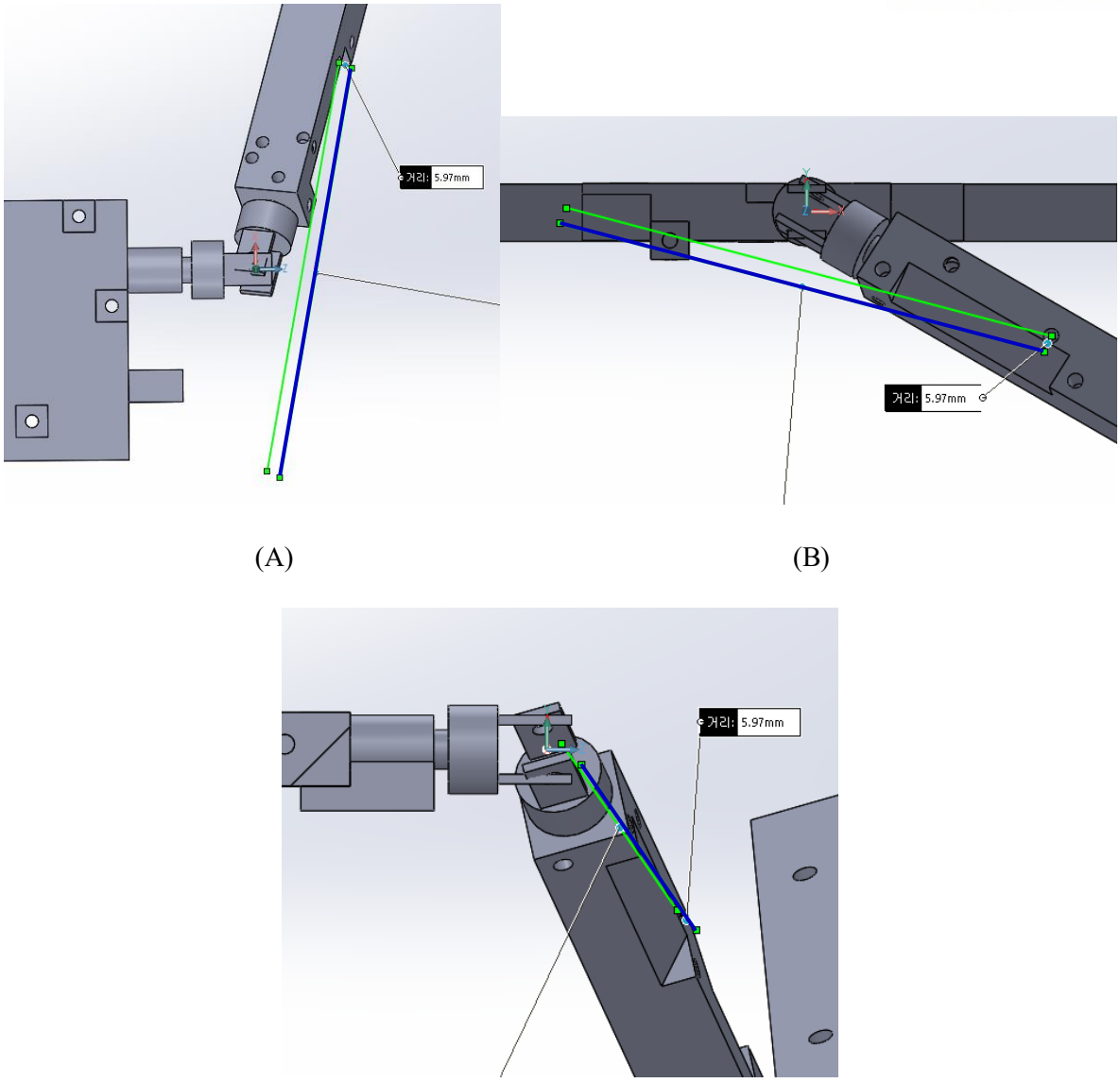

(A) (B)

(C)

Figure 9. Deltoid-posterior (green line), Distance-given (6mm) deltoid-posterior (blue line) in posture 2. (A) Top view. (B) Right side view. (C) Back side view.

It was confirmed that interference occurs between the subscapularis muscle and the upper limb dummy in all postures. In the case of subscapularis muscle, interference continues to occur even if distance is given in the direction of moment arm. So, position the muscle in the opposite direction of the moment arm. In this case, the location of origin & insertion of the muscle is located in the opposite direction to each other relative to the joint center, and the moment value and direction of the joint do not change because the length change of the muscle or the direction of the force does not change (Figure 10).

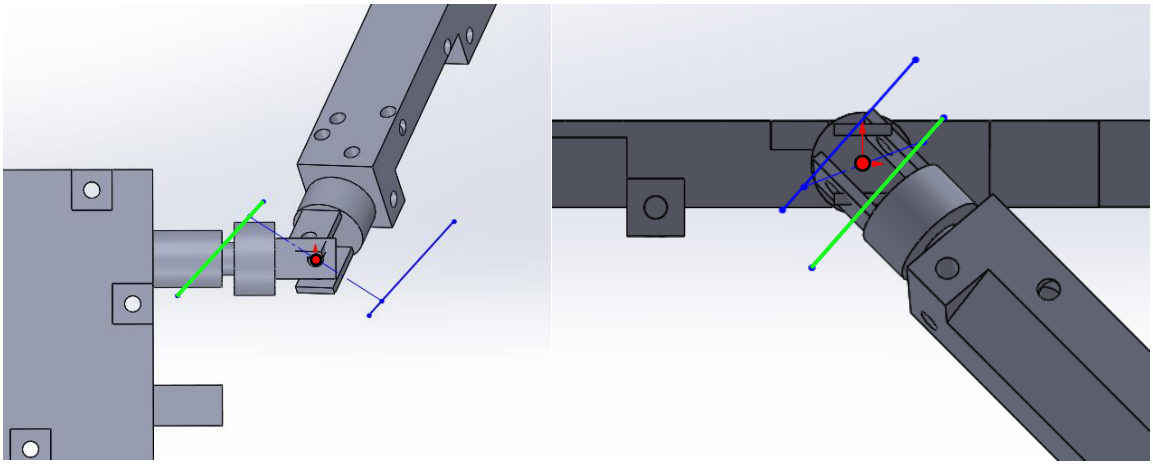

(A) (B)

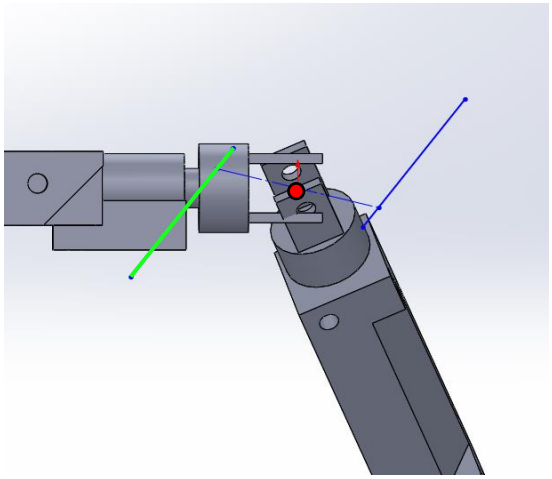

(C)

Figure 10. Subscapularis (green line), Distance-given (opposite direction) subscapularis (blue line) in reference posture. Red dot is shoulder joint. (A) Top view. (B) Right side view. (C) Back side view.

Biceps-long muscles are wrapped around the shoulder, causing interference with the upper limb dummy, and minimizes friction by attaching a roller to the dummy model as shown below (Figure 11).

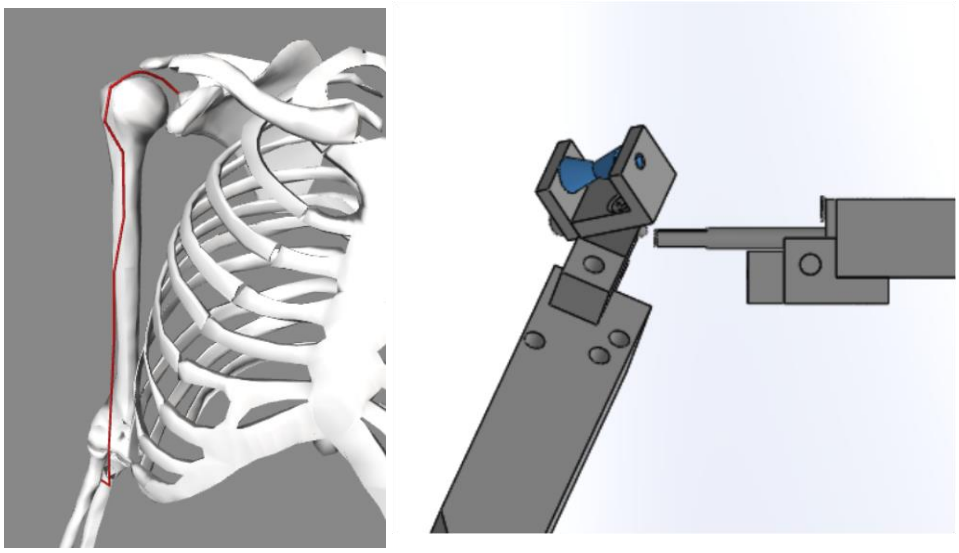

Figure 11. Biceps-long Roller Location

Except for the above 4 muscles (infraspinatus, deltoid-posterior, subscapularis, biceps-long), there is no interference between the upper limb dummy or muscles.

3.2 Parallel elastic element stiffness calculation

Calculate the parallel elastic element stiffness of each muscle to create a spring to replace the muscle. Stiffness can be calculated using the above calculation formula and the fiber length obtained using the OpenSim model. Summarize the stiffness value when moving by the specified range of motion for each posture (Table 10~15). When the optimal fiber length is reduced considering the patient's muscles, the stiffness values are also summarized.

Because the actual muscle does not have a fixed stiffness value and changes, the stiffness value is obtained during the specified range of motion. Through this, the range of moment values of the actual muscle can be obtained. In order to obtain the stiffness value of the muscle that gave the distance, adjust the stiffness value so that the moment value of the muscle that gave the distance is included in the real muscle moment value range, and then obtain the stiffness value. To obtain the stiffness value of Infraspinatus muscles, compare the moment value of the muscles before and after the distance (Figure 12~14).

Table 11. Muscle stiffness in reference posture (Shoulder abduction 25°, shoulder flexion 45°, shoulder external rotation -57.95°, Elbow flexion 60°)

	Muscle	Shoulder Abduction stiffness [N/m]	Shoulder Flexion stiffness [N/m]	Shoulder External rotation stiffness [N/m]
Shoulder	Infraspinatus	1794 ~ 2035	1785 ~ 1847	1785 ~ 1981
	Deltoid-posterior	191 ~ 222	184 ~ 231	201 ~ 212
	Infraspinatus (17.8%)	7221 ~ 10809	8037 ~ 9607	7471 ~ 10455
	Subscapularis (17.8%)	4523 ~ 4954	4558 ~ 4958	4098 ~ 5462
	Pectoralis major-clavicular (17.8%)	480 ~ 531	473 ~ 516	469 ~ 484
Elbow		Elbow Flexion stiffness [N/m]		
	Triceps-long	5860 ~ 7082		
	Biceps-long	575 ~ 746		
	Biceps-short	351 ~ 490		
	Triceps-long (15.9%)	36562 ~ 45804		
	Brachialis (17.8%)	3542 ~ 4655		
	Brachioradialis (17.8%)	465 ~ 745		
	Biceps-long (19.7%)	3195 ~ 5102		
	Biceps-short (19.7%)	2335 ~ 3536		

Table 12 Muscle stiffness in posture 2 (Shoulder abduction 25°, shoulder flexion 60°, shoulder external rotation -71.71°, elbow flexion 60°)

	Muscle	Shoulder Abduction stiffness [N/m]	Shoulder Flexion stiffness [N/m]	Shoulder External rotation stiffness [N/m]
Shoulder	Deltoid-posterior	250 ~ 277	239 ~ 290	258 ~ 270
	Infraspinatus (17.8%)	6033 ~ 7917	6497 ~ 7322	5865 ~ 8181
	Subscapularis (17.8%)	6519 ~ 6690	6556 ~ 6684	5672 ~ 7682
		Elbow Flexion stiffness [N/m]		
Elbow	Triceps-long	7309 ~ 8830		
	Biceps-long	568 ~ 656		
	Biceps-short	396 ~ 554		
	Triceps-long (15.9%)	47551 ~ 59538		
	Brachialis (17.8%)	3542 ~ 4655		
	Brachioradialis (17.8%)	465 ~ 745		
	Biceps-long (19.7%)	2739 ~ 4353		
	Biceps-short (19.7%)	2713 ~ 4124		

Table 13 Muscle stiffness in posture 3 (Shoulder abduction 25°, shoulder flexion 30°, shoulder external rotation -43.31°, elbow flexion 60°)

	Muscle	Shoulder Abduction stiffness [N/m]	Shoulder Flexion stiffness [N/m]	Shoulder External rotation stiffness [N/m]
Shoulder	Infraspinatus	1803 ~ 2418	1805 ~ 2179	1797 ~ 2241
	Deltoid-anterior	1579 ~ 1905	1576 ~ 2190	1620 ~ 1716
	Infraspinatus (17.8%)	8022 ~ 13326	8646 ~ 11743	8637 ~ 12153
	Subscapularis (17.8%)	3550 ~ 4153	3529 ~ 4309	3362 ~ 4421
	Pectoralis major-clavicular (17.8%)	477 ~ 697	492 ~ 690	546 ~ 619
		Elbow Flexion stiffness [N/m]		
Elbow	Triceps-long	4645 ~ 5615		
	Biceps-long	592 ~ 866		
	Biceps-short	356 ~ 497		
	Triceps-long (15.9%)	27734 ~ 34751		
	Brachialis (17.8%)	3542 ~ 4655		
	Brachioradialis (17.8%)	465 ~ 745		
	Biceps-long (19.7%)	3825 ~ 6147		
	Biceps-short (19.7%)	2379 ~ 3604		

Table 14 Muscle stiffness in posture 4 (Shoulder abduction 35°, shoulder flexion 45°, shoulder external rotation -54.37°, elbow flexion 60°)

	Muscle	Shoulder Abduction stiffness [N/m]	Shoulder Flexion stiffness [N/m]	Shoulder External rotation stiffness [N/m]
Shoulder	Deltoid-posterior	185 ~ 195	188 ~ 202	*
	Infraspinatus (17.8%)	5335 ~ 8203	5737 ~ 7514	5512 ~ 7930
	Subscapularis (17.8%)	4463 ~ 4940	4410 ~ 5063	4053 ~ 5442
	Pectoralis major-clavicular (17.8%)	503 ~ 705	511 ~ 697	554 ~ 642
		Elbow Flexion stiffness [N/m]		
Elbow	Triceps-long	6063 ~ 7328		
	Biceps-long	570 ~ 711		
	Biceps-short	459 ~ 644		
	Triceps-long (15.9%)	38073 ~ 47695		
	Brachialis (17.8%)	3542 ~ 4655		
	Brachioradialis (17.8%)	465 ~ 745		
	Biceps-long (19.7%)	3017 ~ 4809		
	Biceps-short (19.7%)	3258 ~ 4972		

Table 15. Muscle stiffness in posture 5 (Shoulder abduction 15°, shoulder flexion 45°, shoulder external rotation 61.02°, elbow flexion 60°)

	Muscle	Shoulder Abduction stiffness [N/m]	Shoulder Flexion stiffness [N/m]	Shoulder External rotation stiffness [N/m]
Shoulder	Infraspinatus	1878 ~ 2570	2126 ~ 2241	1927 ~ 2501
	Deltoid-posterior	218 ~ 246	210 ~ 255	227 ~ 238
	Infraspinatus (17.8%)	9801 ~ 14355	11394 ~ 12152	10109 ~ 13884
	Subscapularis (17.8%)	4590 ~ 4932	4713 ~ 4812	4140 ~ 5456
		Elbow Flexion stiffness [N/m]		
Elbow	Triceps-long	5576 ~ 6740		
	Biceps-long	578 ~ 781		
	Biceps-short	307 ~ 386		
	Triceps-long (15.9%)	34465 ~ 43180		
	Brachialis (17.8%)	3542 ~ 4655		
	Brachioradialis (17.8%)	465 ~ 745		
	Biceps-long (19.7%)	3377 ~ 5402		
	Biceps-short (19.7%)	1743 ~ 2624		

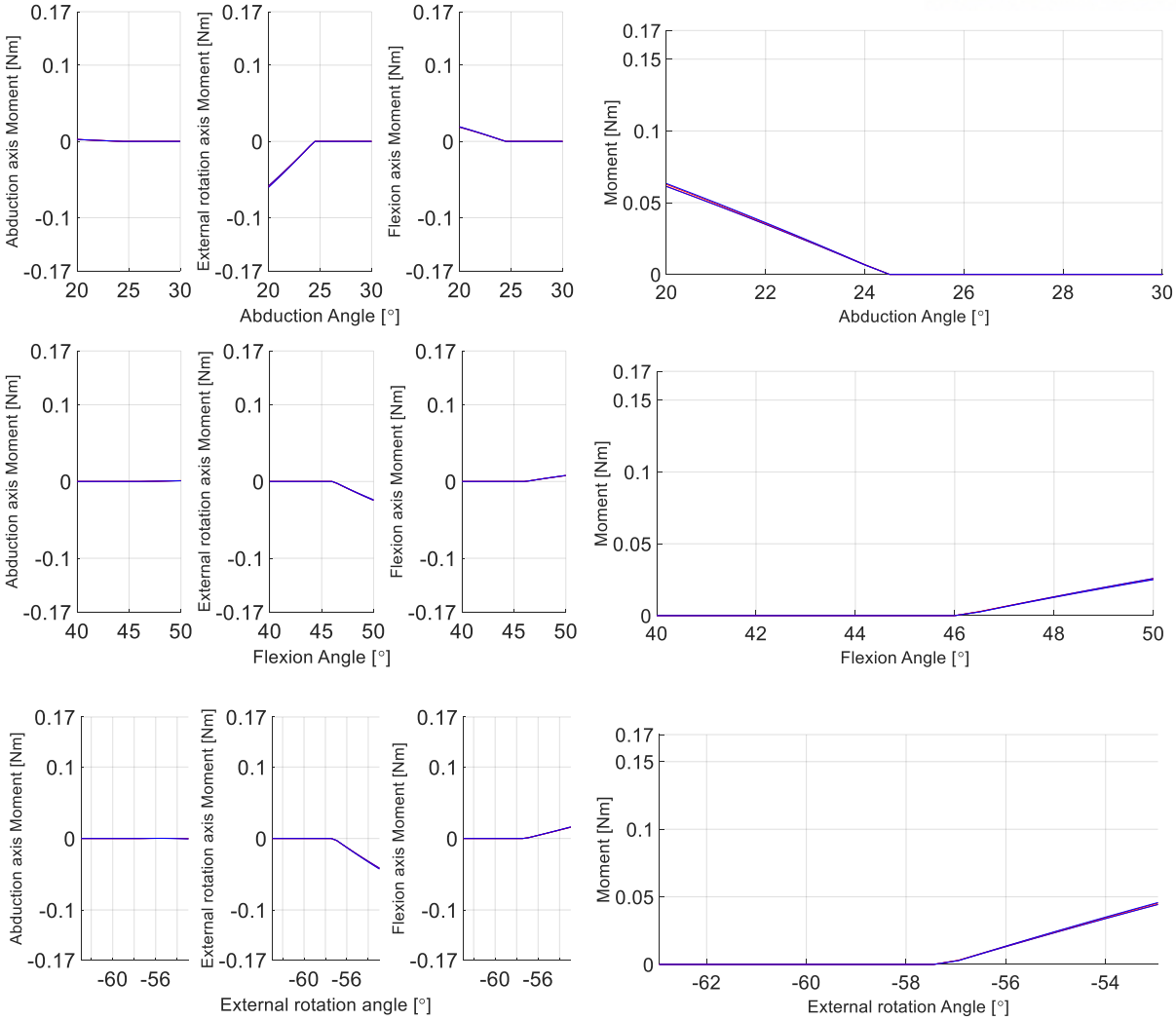

(A) (B)

Figure 12. Infraspinatus moment (blue line, k=1785 ~ 1847 N/m) and distance-given infraspinatus moment (red line, k=1165 ~ 1185 N/m) in reference posture. (A) moment by axis for each movement. (B) moment for each movement.

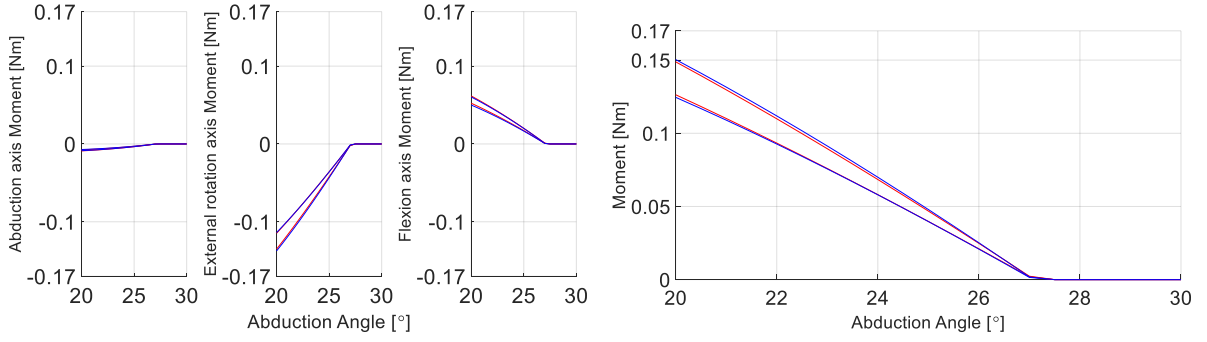

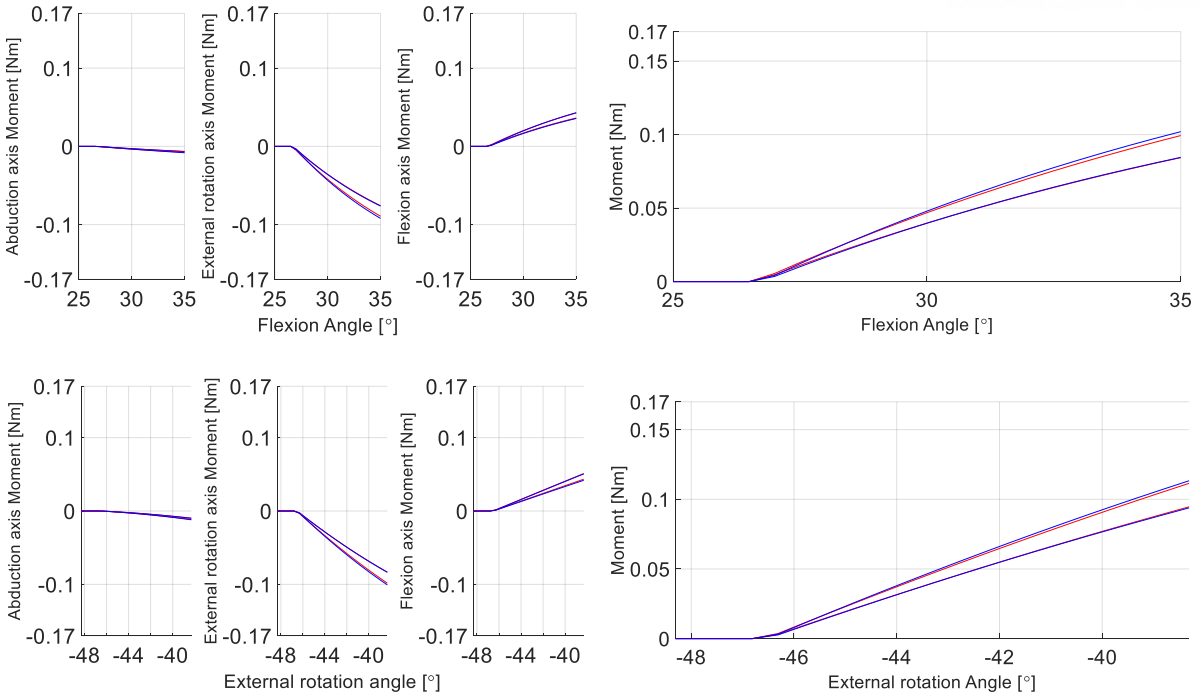

(A) (B)

Figure 13. Infraspinatus moment (blue line, k=1805 ~2179 N/m) and distance-given infraspinatus moment (red line, k=1180 ~ 1400 N/m) in posture 3. (A) moment by axis for each movement. (B) moment for each movement.

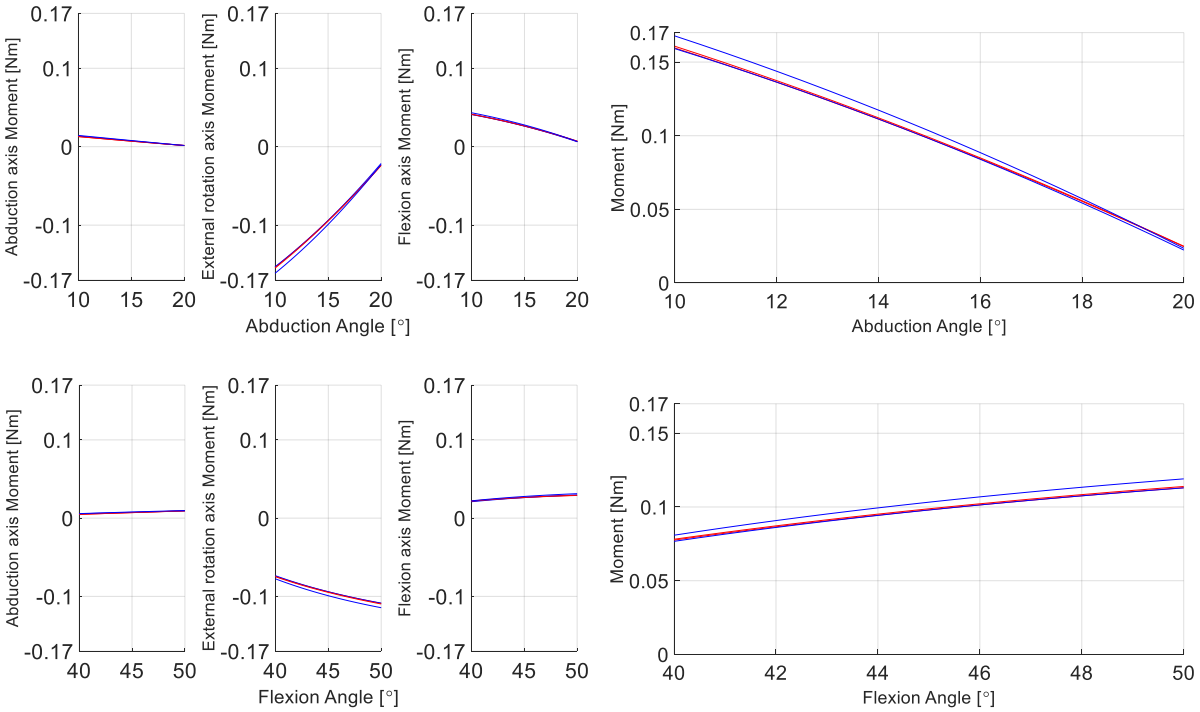

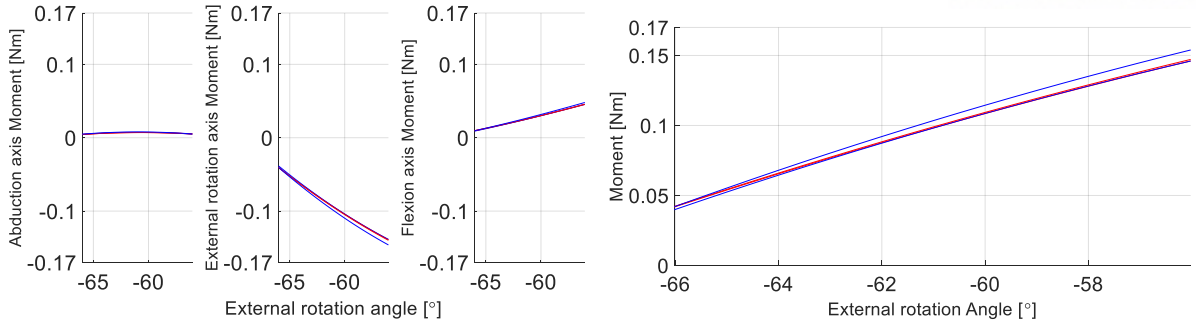

(A) (B)

Figure 14. Infraspinatus moment (blue line, k=2126 ~ 2241 N/m) and distance-given infraspinatus moment (red line, k=1330 ~ 1340 N/m) in posture 5. (A) moment by axis for each movement. (B) moment for each movement.

To obtain the stiffness value of Infraspinatus muscles, which reduced the optimal fiber length by 17.8% to imitate patient muscles, compare the moment value of the muscles before and after the distance (Figure 15~19).

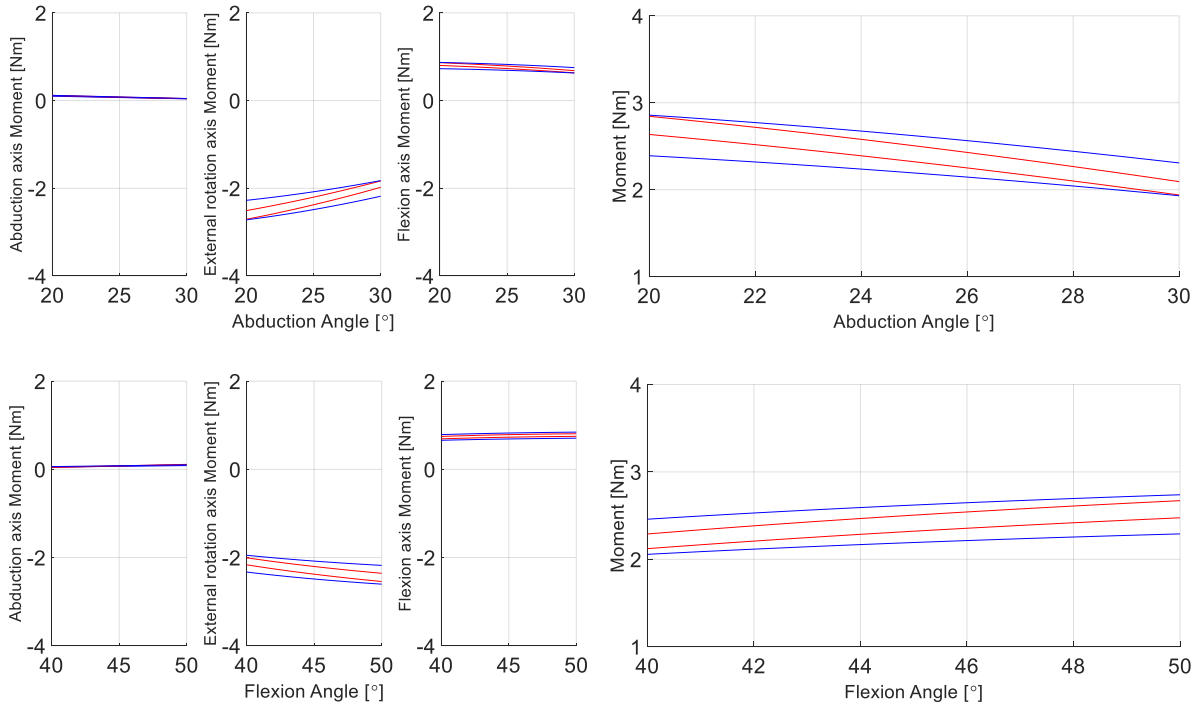

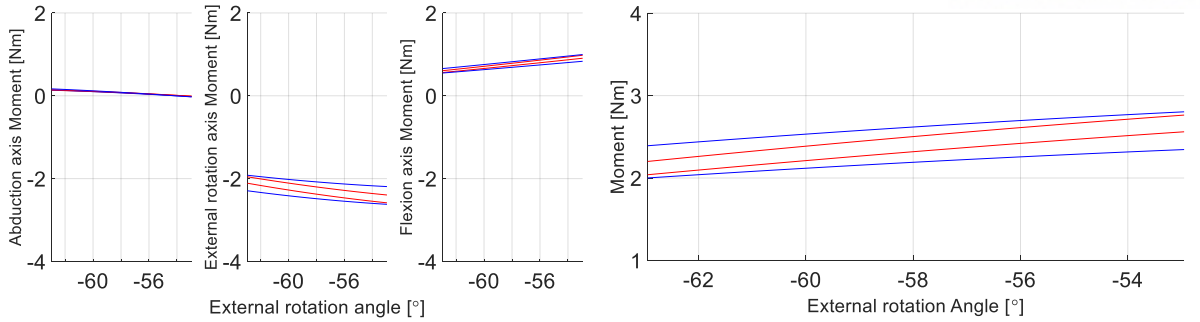

(A) (B)

Figure 15. Infraspinatus moment (blue line, k=8037 ~ 9607 N/m) and distance-given infraspinatus moment (red line, k=6950 ~ 7500 N/m) that reduced optimal fiber length by 17.8% in reference posture. (A) moment by axis for each movement. (B) moment for each movement.

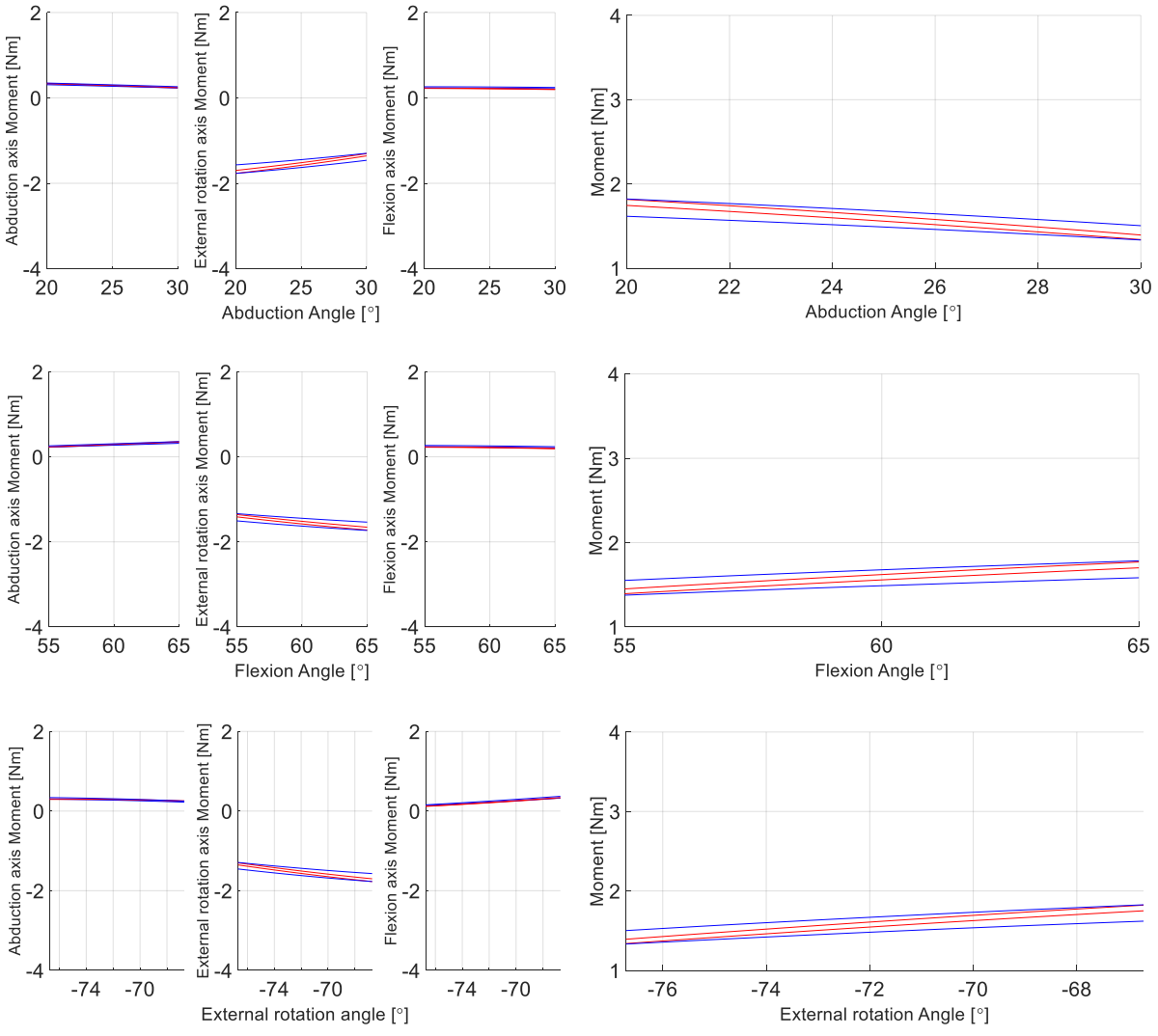

(A) (B)

Figure 16. Infraspinatus moment (blue line, k=6497 ~ 7322 N/m) and distance-given infraspinatus moment (red line, k=5670 ~ 5900 N/m) that reduced optimal fiber length by 17.8% in posture 2. (A) moment by axis for each movement. (B) moment for each movement.

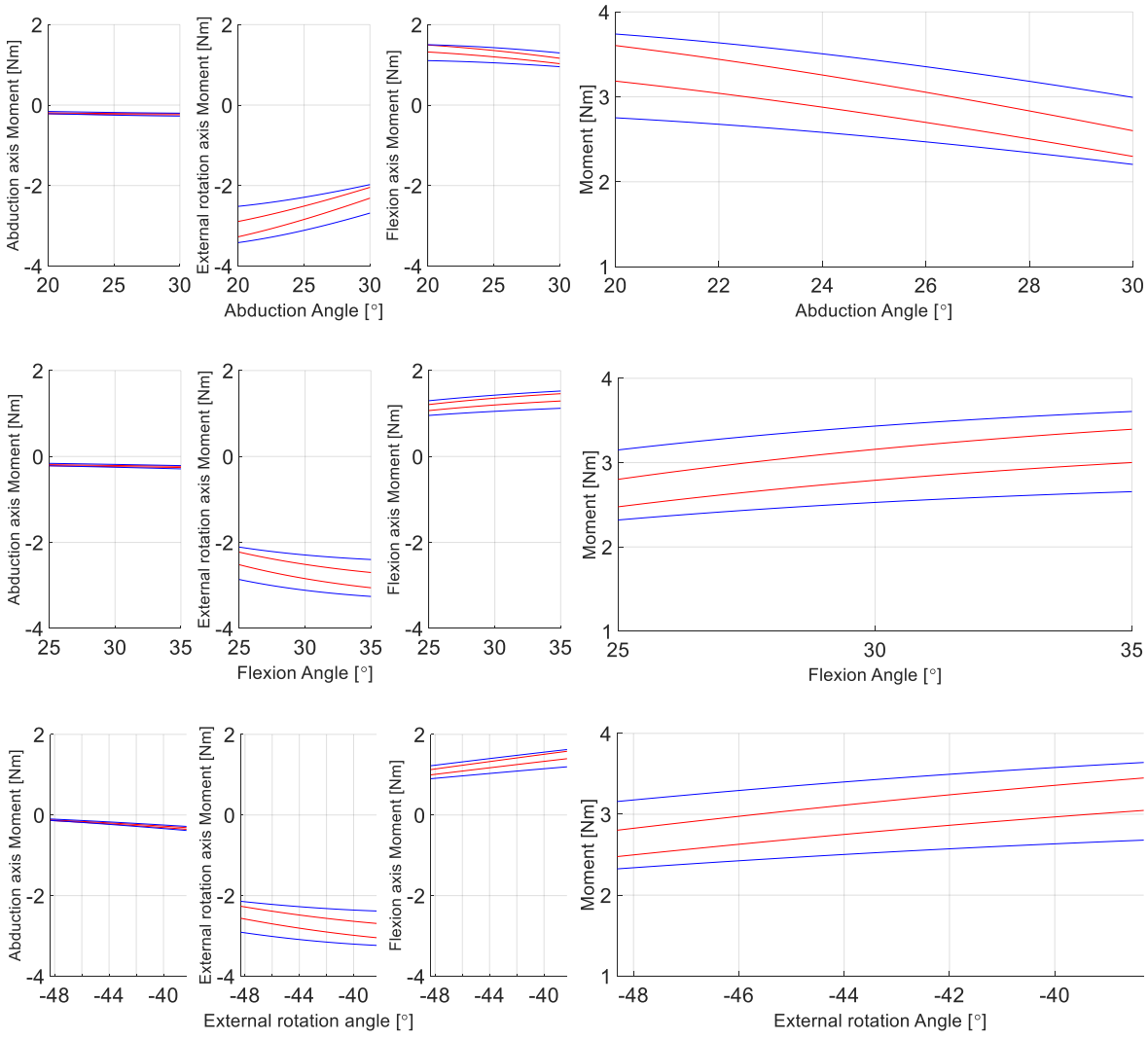

(A) (B)

Figure 17. Infraspinatus moment (blue line, k=8646 ~ 11743 N/m) and distance-given infraspinatus moment (red line, k=7300 ~ 8900 N/m) that reduced optimal fiber length by 17.8% in posture 3. (A) moment by axis for each movement. (B) moment for each movement.

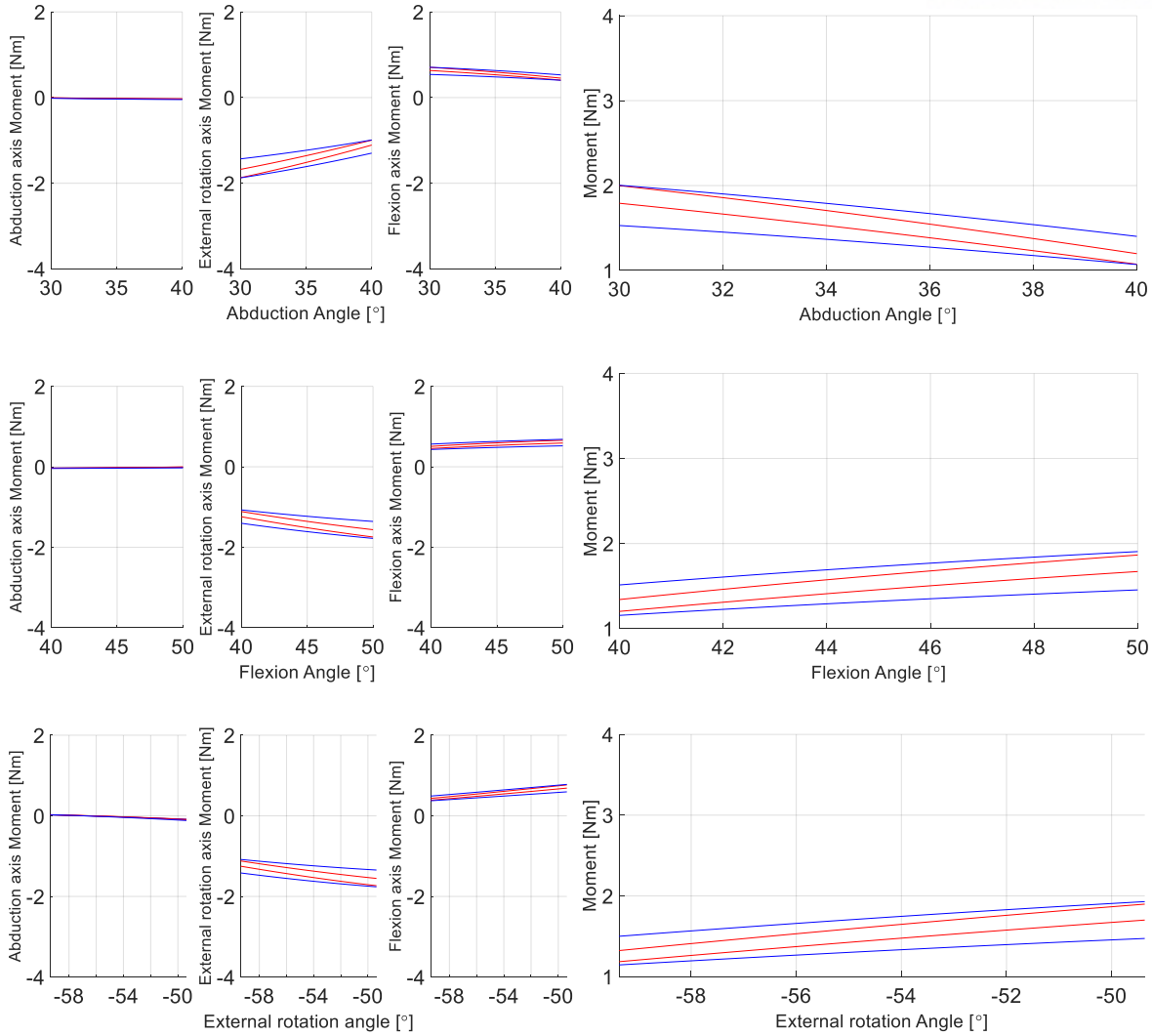

(A) (B)

Figure 18. Infraspinatus moment (blue line, k=5737 ~ 7514 N/m) and distance-given infraspinatus moment (red line, k=5600 ~ 6250 N/m) that reduced optimal fiber length by 17.8% in posture 4. (A) moment by axis for each movement. (B) moment for each movement.

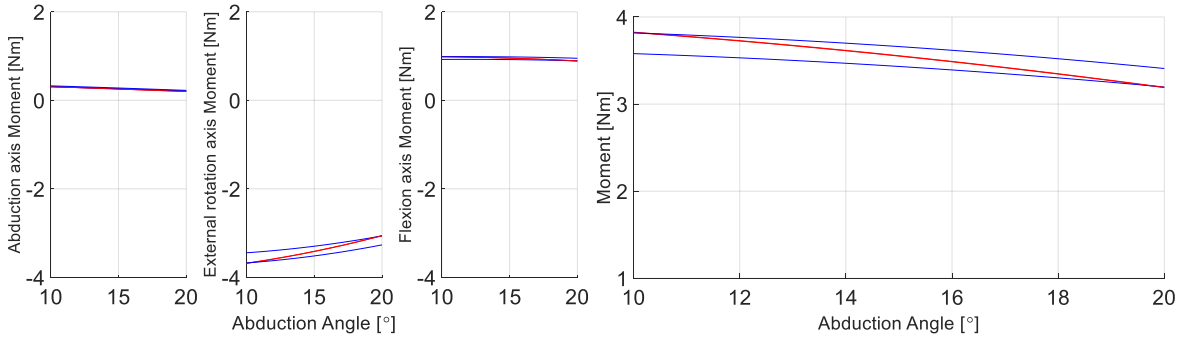

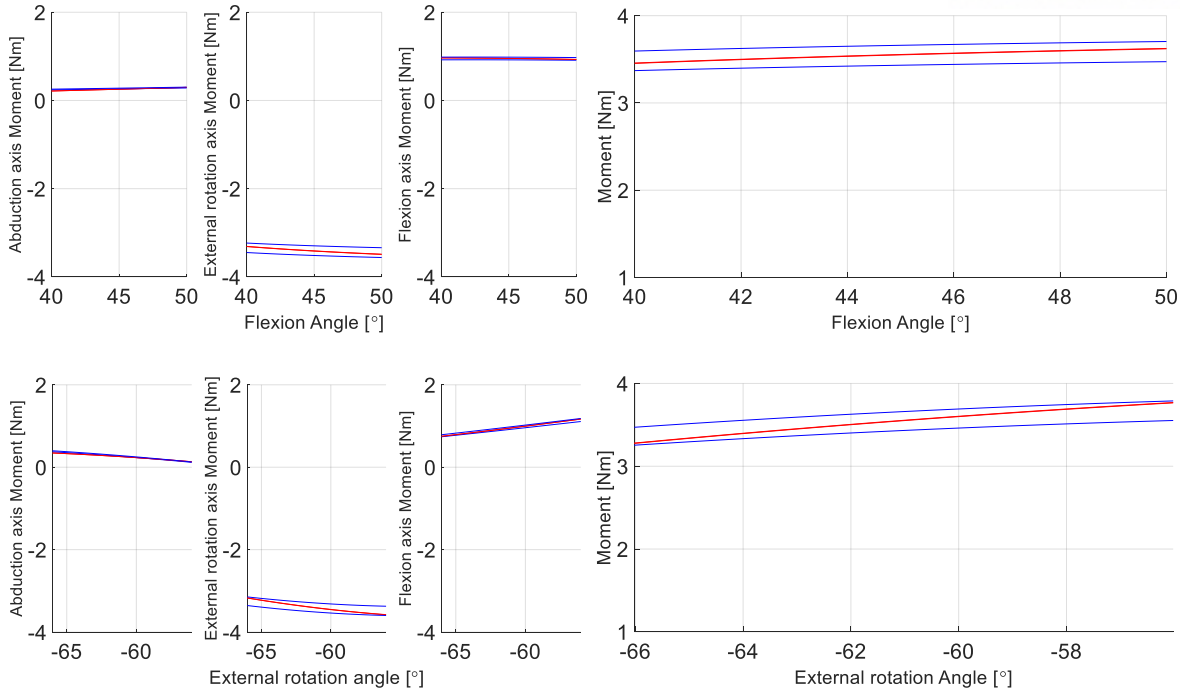

(A) (B)

Figure 19. Infraspinatus moment (blue line, k=11394 ~ 12152 N/m) and distance-given infraspinatus moment (red line, k=9060 ~ 9070 N/m) that reduced optimal fiber length by 17.8% in posture 5. (A) moment by axis for each movement. (B) moment for each movement.

To obtain the stiffness value of Deltoid-posterior muscles, compare the moment value of the muscles before and after the distance. Each range of motion is identified and reflected by the subject's IMU data, which most closely resembles the upper limb dummy's arm length. (shoulder abduction : ±3.5°, shoulder flexion : ±2.5°) (Figure 20).

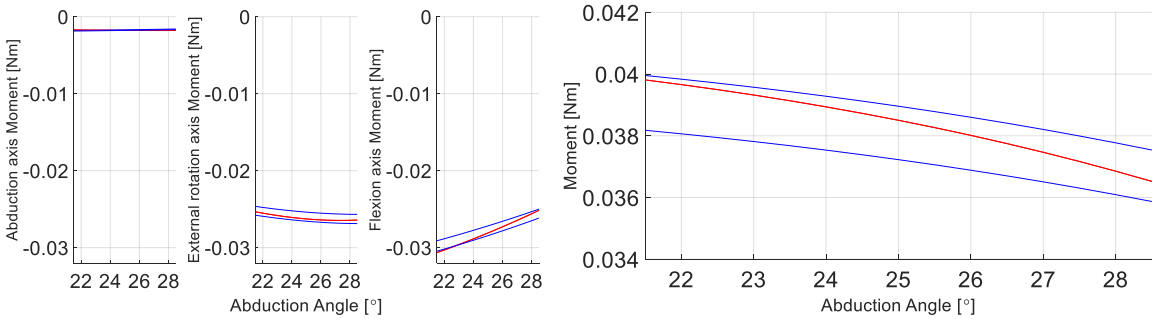

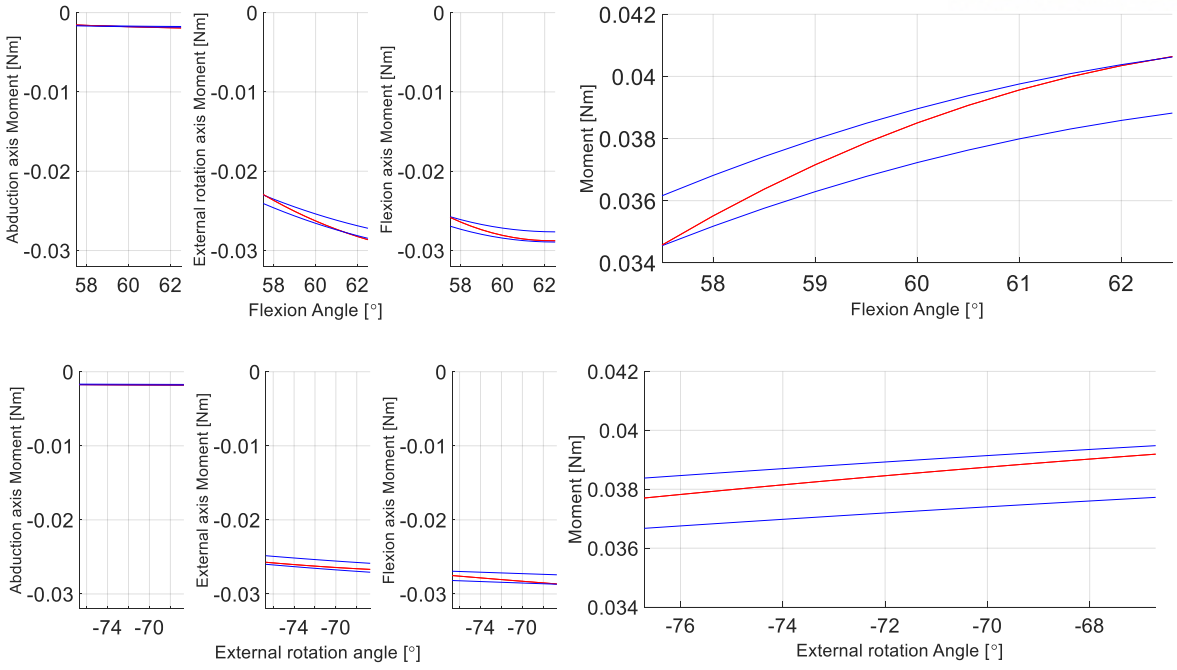

(A) (B)

Figure 20. Deltoid-posterior moment (blue line, k=258 ~ 270 N/m) and distance-given deltoid-posterior moment (red line, k=207 N/m) in posture 2. (A) moment by axis for each movement. (B) moment for each movement.

Organize the stiffness range for each posture including the stiffness range of the distance-given muscles obtained by comparing the moment and the stiffness range obtained by the three movements (Table 16).

Table 16. Orgainze the stiffness range for each posture

	Muscle	Reference posture stiffness, [N/m]	Posture 2 stiffness, [N/m]	Posture 3 stiffness, [N/m]	Posture 4 stiffness, [N/m]	Posture 5 stiffness, [N/m]
Shoulder	Infraspinatus	1165 ~ 1185	*	1180 ~ 1400	*	1330 ~ 1340
	Deltoid-anterior	*	*	1620~1716	*	*
	Deltoid-posterior	201 ~ 212	207	*	188 ~ 195	227 ~ 238

	Infraspinatus (17.8%)	6950 ~ 7500	5670 ~ 5900	7300 ~ 8900	5600 ~ 6250	9060 ~ 9070
	Subscapularis (17.8%)	4558 ~ 4968	6556 ~ 6684	3550 ~ 4153	4463 ~ 4940	4713 ~ 4812
	Pectoralis major-clavicular (17.8%)	473 ~ 484	*	546 ~ 619	554 ~ 642	*
	Triceps-long	5859 ~ 7082	7309 ~ 8830	4645 ~ 5615	6063 ~ 7328	5576 ~ 6740
	Biceps-long	575 ~ 745	568 ~ 656	592 ~ 866	570 ~ 711	578 ~ 781
	Biceps-short	351 ~ 490	396 ~ 554	356 ~ 497	459 ~ 644	307 ~ 386
	Triceps-long (15.9%)	36562 ~ 45804	47551 ~ 59538	27734 ~ 34751	38073 ~ 47695	34465 ~ 43180
Elbow	Brachialis (17.8%)	3542 ~ 4655	3542 ~ 4655	3542 ~ 4655	3542 ~ 4655	3542 ~ 4655
	Brachioradialis (17.8%)	465 ~ 745	465 ~ 745	465 ~ 745	465 ~ 745	465 ~ 745
	Biceps-long (19.7%)	3195 ~ 5102	2739 ~ 4353	3825 ~ 6147	3017 ~ 4809	3377 ~ 5402
	Biceps-short (19.7%)	2335 ~ 3536	2713 ~ 4124	2379 ~ 3604	3258 ~ 4972	1743 ~ 2624

3.3 Upper limb dummy modeling

Scapular & clavicle is set as a fixed frame that does not move and models the main frame to reflect the lengths of humerus and ulna & radius. Shoulder joints are designed as universal joints in consideration of the three-dimensional movement of the shoulder, and elbow joints are designed as hinge joints in consideration of the two-dimensional movement of the elbow. And considering the Origin & Insertion of the muscles, the bars to which the muscles will be connected are fastened to the main frame. The figure below is a three-sided view of the upper limb dummy (Figure 21).

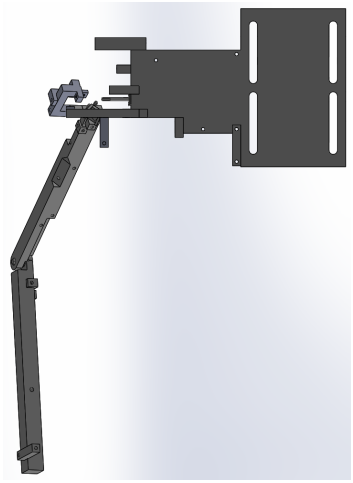

(A)

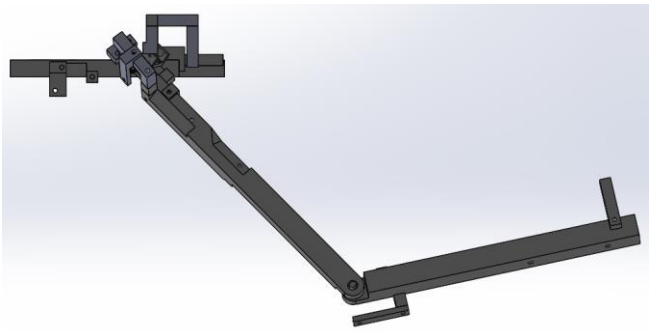

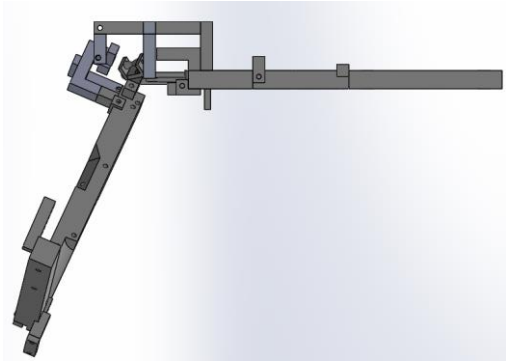

(B) (C)

Figure 21. Three-sided view of upper limb dummy. (A) Top view. (B) Right side view. (C) Front view.

And the base of the upper limb dummy must be able to move in order to pose each pose. A person can pose by changing the position of the chair, but in the case of upper limb dummy, the position of the base must be moved. The range of movement of the upper limb dummy is set by checking the coordinates of the wrist center of the upper limb dummy after each experimental posture and checking the difference between the robot center and the wrist center. (Figure 22; Table 17).

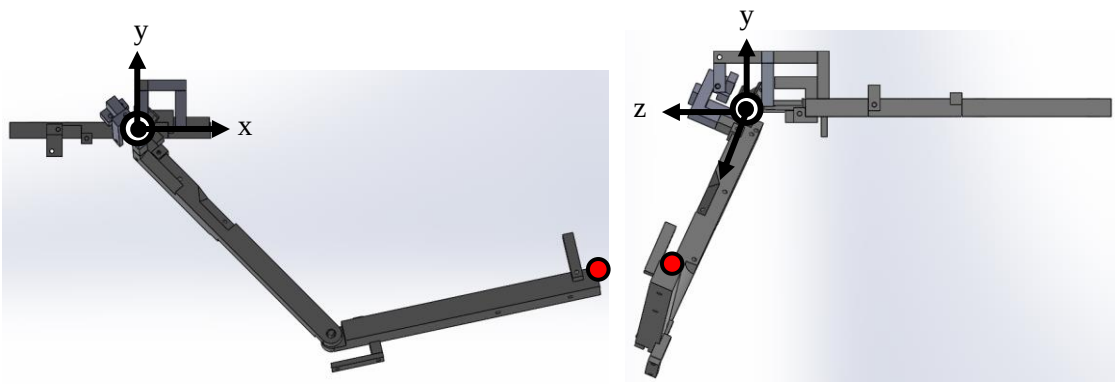

(A) (B)

Figure 22. Upper limb dummy coordinate system & wrist center. Red dot is wrist center. (A) Right side view. (B) Front view.

Table 17. Wrist center coordinates for each posture of upper limb dummy & difference between robot center and wrist center

Posture	Wrist center (based on shoulder joint)			Difference between robot and wrist center		
	X (mm)	Y (mm)	Z (mm)	X (mm)	Y (mm)	Z (mm)
Reference	440.41	-112.13	64.86	0	0	0
Posture 2	456.78	8.45	45	16.37	120.58	-19.86
Posture 3	393.98	-216.17	93.77	53.57	-104.04	28.91
Posture 4	429.43	-97.09	130.03	-10.98	15.04	65.17
Posture 5	442.85	-120.92	-1.71	2.44	-8.79	33.43

The range of movement is designed to move x-axis –54 to 11mm, y-axis –120.8 to 104.2mm, and z-axis –65.2 to 20mm based on the reference position (Figure 23).

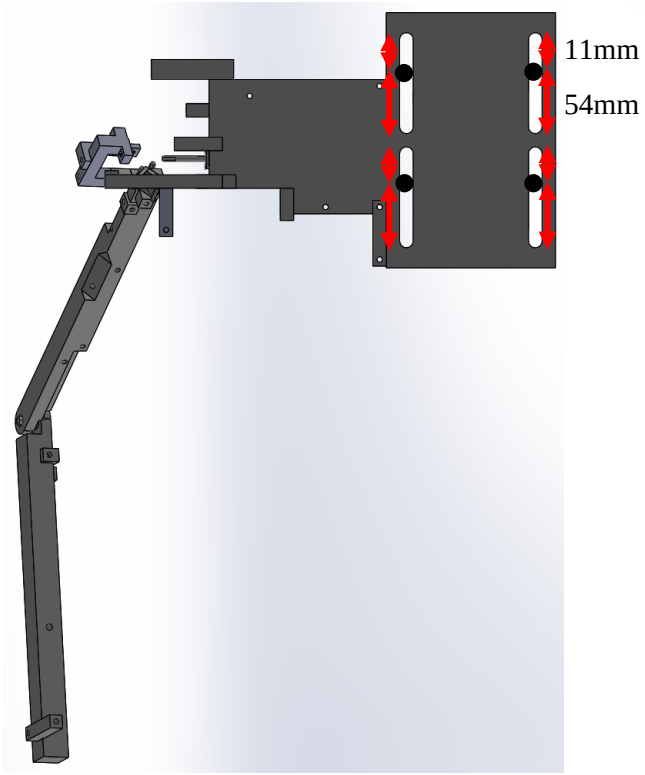

(A)

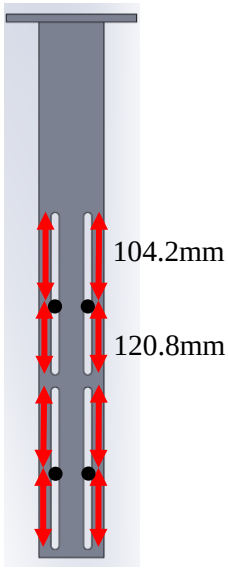

(B)

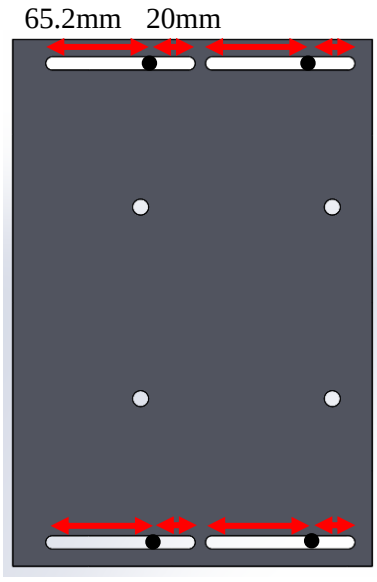

(C)

Figure 23. Upper dummy base moving range. Red line is moving range. Black dot is reference posture fixed position. (A) Range of x-axis movement (-54 to 11mm). (B) Range of y-axis movement (-120.8 to 104.2mm). (C) Range of z-axis movement (-65.2 to 20mm).

Below is a combination of the upper limb dummy and a base for movement. (Figure 24).

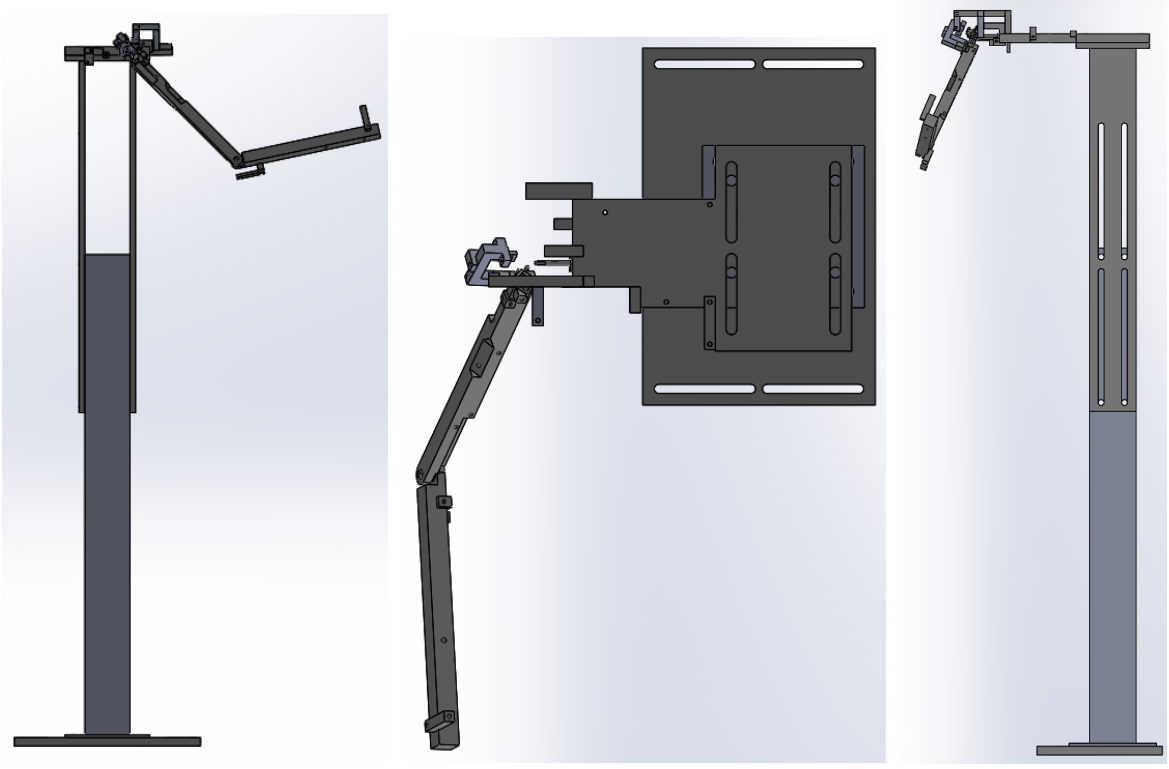

(A) (B) (C)

Figure 24. Upper limb dummy & moving base. (A) Right side view. (B) Top view. (C) Front view.

IV. Discussion

4.1 Necessity of research

The purpose of this study is to explore the design method of 3DOF upper limb dummy including shoulder and elbow muscles and joints for mechanical impedance analysis of upper limb. There are some limitations to the measurement of spasticity currently used in clinical practice. Since it is mostly a manual examination, it relies on the evaluator's hand sensation and experience, and results may vary depending on the evaluator. Also, only one joint can be examined, and quantitative evaluation is difficult. And most of the upper limb models presented in the existing papers are those that can only be moved in two dimensions, not in three dimensions, and are simulated models that are not actually manufactured. The actual purpose of the 2DOF or 3DOF upper limb model is also mostly related to the control of the model, unlike the purpose of this study. Studies on the analysis of mechanical impedance at the upper limb have been conducted in a small number of limited laboratories worldwide, including MIT, and yet these studies are only limited studies at the initial laboratory level. And most of the studies related to this have performed mechanical impedance measurement for the upper limb 2 degrees of freedom (or 2 joints). In this study, it is thought that it will contribute to the analysis of the upper limb impedance

for 3 degrees of freedom by exploring a dummy design method for the analysis of the upper limb joint impedance in 3 degrees of freedom.

4.2 summary

The design was sought in consideration of shoulder and elbow joint movements in three-dimensional space and the wrist joint was not considered. Prioritize muscles by determining the relative torque of individual muscles to imitate the major muscle groups (Table 1). The muscle parameters used to obtain the torque value were investigated in various papers and the average value was used to increase accuracy. The main muscles obtained through calculation are compared with the main muscles presented in the existing literature to increase reliability. We don't need to consider all muscles because the goal is to design a dummy to measure upper limb impedance rather than individual muscle observation. Accordingly, the screening process of muscles was performed. First, muscles with small contribution to shoulder and elbow movement (Coracobrachialis, Pronator teres, Anconeus) are excluded. Muscles that function like other muscles but lack their role (Teres major, Teres minor, Triceps-lateral) are also considered to be unnecessary. In addition, the necessary muscles were selected for the impedance comparison analysis between the patient and the normal person through previous papers on the treatment of stroke patients. All of these processes were conducted through advisory conference with clinical experts, so the results of muscle selection have credibility (Table 6).

When selecting an experimental posture, a posture with a resistance torque of 0 was selected as a reference posture through prior studies. However, the previous study conducted a study on 2D plane motion (shoulder horizontal adduction, elbow flexion, wrist flexion). So, in order to select the posture for the rest of the movements (shoulder abduction, shoulder external rotation), the person directly took a posture and measured. It was confirmed that the maximum angle of shoulder abduction that can be taken by the upper limb impedance measurement robot currently possessed by our laboratory is 40° for men (height 179 cm) and 50° for women (height 159 cm). Based on this, it was found that the smaller the height, the greater the shoulder abduction angle. So, the reference shoulder abduction angle is set to 25°, which is less than the maximum male shoulder abduction angle (Fig 1). The upper limb impedance measuring robot connect the human arm through the gimbal, and the upper limb dummy will also be connected through the gimbal. The gimbal allows the x, y, and z axes to move freely and allow the person to take the most natural posture when energized. For this reason, the shoulder external rotation angle is automatically set when the shoulder abduction and shoulder horizontal adduction angles are determined. Thus, the shoulder and wrist coordinates of the person with similar arm length to the upper limb dummy are used to specify the Shoulder external rotation angle. To specify the angle of different postures through that method.

In addition, since it is a posture applied to an actual human experiment, it should be easy to verify whether the subject has properly taken the posture. So, after taking the posture, the angle for each posture is summarized by the shoulder abduction angle seen from the front and the shoulder flexion angle seen from the side (Table 7).

Our upper limb dummy model aims to analyze the mechanical impedance of the upper limb by observing the passive movement of the muscles. Passive force is generated in the passive movement of the muscle, which causes a moment in the joint. Passive forces are created by parallel elastic elements. Parallel elastic element stiffness can be obtained through the relationship between passive force and muscle length. When the muscle length is shorter than the optimal fiber length, passive force does not occur (Fig 4). By using the parallel elastic stiffness value for the spring constant of the spring, a spring that mimics the passive movement of the muscle can be produced. Parallel elastic element stiffness depending on muscle length, optimal fiber length, and maximum isometric muscle force, and optimal fiber length and maximum isometric muscle force experimentally obtained in previous studies are intrinsic values of each muscle and do not change (Table 8). The value that affects the parallel eastic element stiffness of the muscle is the length of the muscle. The length of the muscle was obtained through the OpenSim model. In the case of stroke patients, the muscles stiffen and contract, causing the arm to bend toward the body. This phenomenon increases muscle resistance, which means that parallel elastic element stiffness increases. Prior paper was investigated to check the increase in stiffness, and the optimal fiber length in patients decreased by 19.7% for biceps brachii and 15.9% for triceps brachii compared to normal subjects. The remaining muscles are assumed to decrease by 17.8%, the average of the two values.

Selected muscles do not have parallel elastic element stiffness in all poses. If the length of the muscle is shorter than the optimal fiber length in the posture, the muscle is in a stretched state and passive force does not occur. Therefore, when the specified movement is applied in each position, the length of the muscle is checked, and if the muscle is shorter than the optimal fiber length, the muscle is excluded from that position (Table 8). Subsequently, inter-muscular interference is investigated in each position. Interference between infraspinatus and origin of triceps-long occurs in all postures. Give at least 5mm of distance to the origin & insert of the muscle in consideration of turning the muscle into a spring (Fig 7). To reduce the difference of moment arm and moment as much as possible, the distance was given in the direction of moment arm around the shoulder point in the reference position. Deltoid-posterior muscles interfere with the humerus frame in position 2, giving a distance in the same way (Fig 8). Subscapularis creates interference in all postures and continues to interfere even if you give distance in the direction of the moment arm. So, it moves the muscle in the opposite direction of the moment arm. In this case, the origin & insertion of the muscle is located in the opposite direction around the shoulder joint. Since the two coordinates are completely opposite, the moment arm and the length change of the

muscle according to the movement are the same. And because both the direction of the force and the direction of the moment arm change in the opposite direction, the value of the moment and the direction become the same. The biceps-long muscle wraps around the shoulder, causing friction with the shoulder joint. To minimize this, rollers are installed in the path. For the location of the roller, refer to the coordinates provided in the OpenSim model.

The parallel elastic element stiffness of each posture is calculated using the passive force calculation formula. The length of the muscle varies with movement, and the parallel elastic element stiffness varies with the length of the muscle. Therefore, we obtain a passive strain range. The parallel elastic element stiffness is also obtained when the optimal fiber length is reduced considering the muscles of stroke patients (Table 9). However, since the obtained stiffness is the stiffness of the muscle that did not distance, the stiffness of the muscle that gave the distance must be determined separately. It is calculated by comparing the moment of the muscle that did not distance and the moment after the distance. The stiffness is arbitrarily specified so that the moment of the muscle that gave the distance is included within the range determined by the stiffness of the existing muscle, and the stiffness at that time is obtained. The stiffness range of the existing muscles sets the range that is included in all of the stiffness calculated during the three movements. Therefore, the stiffness of the muscles that gave distance is also included in the stiffness of all three movements. Infraspinatus gave distance at the basic position, and in all positions, the moment is included in the moment of the existing muscle, so we can use the distance-given muscle in other positions. In the early case of deltoid-posterior, the moment of the distance-given muscle was outside the range of the moment of the existing muscle. This was thought to be because the randomly selected range of motion was larger than the range of motion in the analysis of the actual impedance. So, through the experimental data conducted in our laboratory, the actual range of motion of a person similar to the arm length of the upper limb dummy was confirmed (shoulder abduction : ±3.5°, shoulder flexion : ±2.5°). However, the moment was still outside the range of the moment of the existing muscle. So, we increased the muscles' origin & insert by 40mm each in the direction of the muscles' length and were able to match the moment value (Figure 25).

The main frame of the upper dummy consists of three parts: Scapular & Clavicle, Humerus, and Ulna & Radius. Scapular & Clavicle is a part that will be fixed to the base, so there is no movement, so it is designed as one part. Ulna & Radius is designed as a part because it does not consider the pronation/supination movement. Shoulder joints are designed as universal joints because they must be capable of three-dimensional motion. Elbow joint is designed as a hinge joint. Fixed the bars to the main frame to avoid interference with each other in line with the origin & insert of the selected muscles. The base must be movable in order to the upper limb dummy to take each position. To this end, the difference between the wrist center of the upper limb dummy for each posture and the center of the impedance measuring robot is checked, and a base that can move the distance by the difference is

designed.

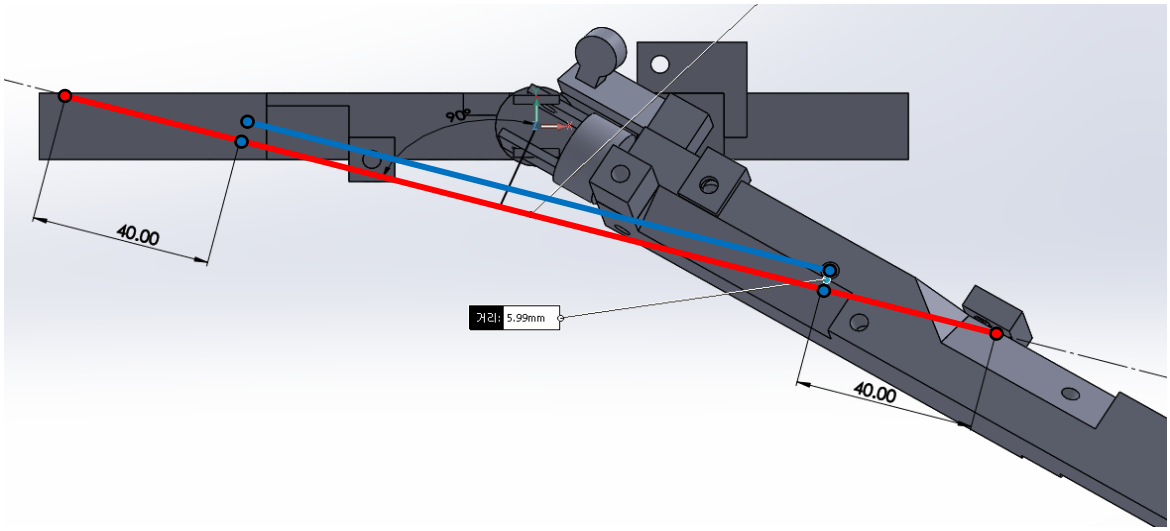

Figure 25. Deltoid-posterior muscle in posture 2. Red line is muscle with increased length (origin & insert by 40mm each in the direction of the muscles' length) after distance (6mm). Blue line is normal deltoid-posterior muscle.

4.3 Expectation of research

This study is thought to contribute greatly to the creation of a 3DOF upper limb dummy for upper limb impedance analysis. Also, it will be helpful to make a spring that imitate muscles using parallel elastic element stiffness obtained for each posture. It is believed that impedance analysis will be possible using the impedance measuring robot and the upper limb dummy that produced based on this study. In addition, it is thought that the impedance tendency analysis of the normal person and the patient will be possible by replacing the spring made using the parallel elastic element stiffness of the stroke patient with the spring made using the normal parallel elastic element stiffness. Furthermore, there is a possibility that it may serve as a training aids for clinical tests (Modified Ashworth Scale, Tardieu Scale, etc.) performed by the hands of medical staff to measure the stiffness of current stroke patients.

References

1. Mussa-Ivaldi, F. A., Hogan, N., & Bizzi, E. (1985). Neural, mechanical, and geometric factors subserving arm posture in humans. Journal of Neuroscience, 5(10), 2732-2743.
2. Dolan, J. M., Friedman, M. B., & Nagurka, M. L. (1993). Dynamic and loaded impedance components in the maintenance of human arm posture. IEEE transactions on systems, man, and cybernetics, 23(3), 698-709.
3. Tsuji, J. (1995). Palladium reagents and catalysts. Wiley & sons.
4. Gomi, H., & Kawato, M. (1997). Human arm stiffness and equilibrium-point trajectory during multi-joint movement. Biological cybernetics, 76(3), 163-171.
5. Acosta, A. M., Kirsch, R. F., & Perreault, E. J. (2000). A robotic manipulator for the characterization of two-dimensional dynamic stiffness using stochastic displacement perturbations. Journal of Neuroscience Methods, 102(2), 177-186.
6. Palazzolo, J. J., Ferraro, M., Krebs, H. I., Lynch, D., Volpe, B. T., & Hogan, N. (2007). Stochastic estimation of arm mechanical impedance during robotic stroke rehabilitation. IEEE Transactions on Neural Systems and Rehabilitation Engineering, 15(1), 94-103.
7. Palastanga, N., & Soames, R. (2011). Anatomy and human movement, structure and function with PAGEBURST access, 6: anatomy and human movement. Elsevier Health Sciences.
8. Stone, R. J., & Stone, J. A. (2003). Atlas of skeletal muscles. McGraw-Hill.
9. Perotto, A. O. (2011). Anatomical guide for the electromyographer: the limbs and trunk. Charles C Thomas Publisher.
10. Feneis, H., & Dauber, W. (2000). Pocket Atlas of Human Anatomy. Thieme.
11. Braune, W., & Fischer, O. (1889). Die rotationsmomente der beugemuskeln am ellenbogengelenk des menschen. Hirzel.
12. Da Corte, D. (2014). Biomechanical analysis of the sidestep cutting maneuver in football players with OpenSim.
13. Maganaris, C. N., & BALZOPOULOS, V. (2000). In Vivo mechanics of maximum isometric muscle contraction in man: Implications for modeling-based estimates of muscle specific tension, [in:] W. Herzog (ed.) Skeletal muscle mechanics. Skeletal muscle mechanics: from mechanisms to function. Wiley & Sons Ltd, 267-288.
14. Sacks, R. D., & Roy, R. R. (1982). Architecture of the hind limb muscles of cats: functional

significance. Journal of Morphology, 173(2), 185-195.

15. Kuechle, D. K., Newman, S. R., Itoi, E., Morrey, B. F., & An, K. N. (1997). Shoulder muscle moment arms during horizontal flexion and elevation. Journal of Shoulder and Elbow Surgery, 6(5), 429-439.

16. Kuechle, D. K., Newman, S. R., Itoi, E., Niebur, G. L., Morrey, B. F., & An, K. N. (2000). The relevance of the moment arm of shoulder muscles with respect to axial rotation of the glenohumeral joint in four positions. Clinical Biomechanics, 15(5), 322-329.

17. Favre, P., Sheikh, R., Fucentese, S. F., & Jacob, H. A. (2005). An algorithm for estimation of shoulder muscle forces for clinical use. Clinical biomechanics, 20(8), 822-833.

18. Veeger, H. E. J., Van der Helm, F. C. T., Van Der Woude, L. H. V., Pronk, G. M., & Rozendal, R. H. (1991). Inertia and muscle contraction parameters for musculoskeletal modelling of the shoulder mechanism. Journal of biomechanics, 24(7), 615-629.

19. Veeger, H. E. J., Yu, B., An, K. N., & Rozendal, R. H. (1997). Parameters for modeling the upper extremity. Journal of biomechanics, 30(6), 647-652.

20. Wood, J. E., Meek, S. G., & Jacobsen, S. C. (1989). Quantitation of human shoulder anatomy for prosthetic arm control—I. Surface modelling. Journal of biomechanics, 22(3), 273-292.

21. Langenderfer, J., Jerabek, S. A., Thangamani, V. B., Kuhn, J. E., & Hughes, R. E. (2004). Musculoskeletal parameters of muscles crossing the shoulder and elbow and the effect of sarcomere length sample size on estimation of optimal muscle length. Clinical Biomechanics, 19(7), 664-670.

22. An, K. N., Hui, F. C., Morrey, B. F., Linscheid, R. L., & Chao, E. Y. (1981). Muscles across the elbow joint: a biomechanical analysis. Journal of biomechanics, 14(10), 659-669.

23. Murray, W. M., Delp, S. L., & Buchanan, T. S. (1995). Variation of muscle moment arms with elbow and forearm position. Journal of biomechanics, 28(5), 513-525.

24. Murray, W. M., Buchanan, T. S., & Delp, S. L. (2000). The isometric functional capacity of muscles that cross the elbow. Journal of biomechanics, 33(8), 943-952.

25. Murray, W. M., Buchanan, T. S., & Delp, S. L. (2002). Scaling of peak moment arms of elbow muscles with upper extremity bone dimensions. Journal of biomechanics, 35(1), 19-26.

26. Amis, A. A., Dowson, D., & Wright, V. (1979). Muscle strengths and musculoskeletal geometry of the upper limb. Engineering in medicine, 8(1), 41-48.

27. Buchanan, T. S. (1995). Evidence that maximum muscle stress is not a constant: differences in specific tension in elbow flexors and extensors. Medical engineering & physics, 17(7), 529-536.

28. Chang, Y. W., Hughes, R. E., Su, F. C., Itoi, E., & An, K. N. (2000). Prediction of muscle force involved in shoulder internal rotation. Journal of Shoulder and Elbow Surgery, 9(3), 188-195.

29. Crowninshield, R. D., & Brand, R. A. (1981). A physiologically based criterion of muscle force prediction in locomotion. Journal of biomechanics, 14(11), 793-801.

30. Lippert, L. (2011). Clinical Kinesiology and Anatomy: FA Davis Company.

31. Nalysnyk, L., Papapetropoulos, S., Rotella, P., Simeone, J. C., Alter, K. E., & Esquenazi, A. (2013). OnabotulinumtoxinA muscle injection patterns in adult spasticity: a systematic literature review. BMC neurology, 13(1), 118.

32. Jagodnik, K. M., & van den Bogert, A. J. (2010). Optimization and evaluation of a proportional derivative controller for planar arm movement. Journal of Biomechanics, 43(6), 1086-1091.

33. Zadravec, M., & Matjačić, Z. (2013). Planar arm movement trajectory formation: an optimization based simulation study. Biocybernetics and Biomedical Engineering, 33(2), 106-117.

34. Sharifi, M., Salarieh, H., & Behzadipour, S. (2017). Nonlinear optimal control of planar musculoskeletal arm model with minimum muscles stress criterion. Journal of Computational and Nonlinear Dynamics, 12(1).

35. Oatis, C. A. (2016). Kinesiology: the mechanics and pathomechanics of human movement. Lippincott Williams & Wilkins.

36. Floyd, R. T.; THOMPSON, Clem W. (2017). Manual of Structural Kinesiology.

37. Foster, M. A. (2019). Therapeutic kinesiology: musculoskeletal systems, palpation, and body mechanics. Pearson Higher Ed.

38. Ren, Y., Kang, S. H., Park, H. S., Wu, Y. N., & Zhang, L. Q. (2012). Developing a multi-joint upper limb exoskeleton robot for diagnosis, therapy, and outcome evaluation in neurorehabilitation. IEEE Transactions on Neural Systems and Rehabilitation Engineering, 21(3), 490-499.

39. Thelen, D. G. (2003). Adjustment of muscle mechanics model parameters to simulate dynamic contractions in older adults. J. Biomech. Eng., 125(1), 70-77.

40. Saul, K. R., Hu, X., Goehler, C. M., Vidt, M. E., Daly, M., Velisar, A., & Murray, W. M. (2015). Benchmarking of dynamic simulation predictions in two software platforms using an upper limb musculoskeletal model. Computer methods in biomechanics and biomedical engineering, 18(13), 1445-1458.

41. Nelson, C. M., Murray, W. M., & Dewald, J. P. (2018). Motor Impairment–Related Alterations in Biceps and Triceps Brachii Fascicle Lengths in Chronic Hemiparetic Stroke. Neurorehabilitation and neural repair, 32(9), 799-809.

42. Holzbaur, K. R., Murray, W. M., & Delp, S. L. (2005). A model of the upper extremity for simulating musculoskeletal surgery and analyzing neuromuscular control. Annals of biomedical engineering, 33(6), 829-840.

43. McConville, J. T., Clauser, C. E., Churchill, T. D., Cuzzi, J., & Kaleps, I. (1980). Anthropometric relationships of body and body segment moments of inertia. ANTHROPOLOGY RESEARCH PROJECT INC YELLOW SPRINGS OH.

44. Saul, K. R., Hu, X., Goehler, C. M., Vidt, M. E., Daly, M., Velisar, A., & Murray, W. M. (2015). Benchmarking of dynamic simulation predictions in two software platforms using an upper limb musculoskeletal model. Computer methods in biomechanics and biomedical engineering, 18(13), 1445-1458.

Acknowledgement

To me who is having a hard time adjusting to research after entering graduate school, the Robotics & Rehabilitation Engineering Laboratory that helped me with my studies and research life is a place where I was very thankful and learned a lot. Therefore, I would like to express my gratitude to those who have helped and supported a lot during the graduate school master's course.

First of all, I would like to thank Professor Sang Hoon Kang who was my advisor. I was able to finish my master's degree because of your advice on life in the lab after entering graduate school and your guidance on future plans and research progress. Also, I would like to express my sincere appreciation to Professor Namhun Kim and Professor Gwanseob Shin for evaluating my thesis and giving good comments until the thesis was completed.

I would like to sincerely thanks Dr. Sung Shin Kim for always saying good words and helping me during the lab life, and Hyunah Kang for helping me to adjust to lab and helping me research. Also, I sincerely thank all of Seongil Hwang, Chansong Park, and JeongWoo Son who helped me in various ways until the thesis was completed.

I was able to spend my graduate life well after meeting a kind and good colleague. Thank you for making me have a pleasant graduate life, and I was happy thanks to my lab colleagues.

Lastly, I would like to thank my parents for trusting and supporting my career path. Lab life was a really valuable experience in my life, and I will try to develop further based on it.